



(12)

# Oversættelse af europæisk patentskrift

Patent- og  
Varemærkestyrelsen

(51) Int.Cl.: **A 61 K 45/00 (2006.01)**

(45) Oversættelsen bekendtgjort den: **2018-01-08**

(80) Dato for Den Europæiske Patentmyndigheds  
bekendtgørelse om meddelelse af patentet: **2017-09-27**

(86) Europæisk ansøgning nr.: **08854580.1**

(86) Europæisk indleveringsdag: **2008-11-26**

(87) Den europæiske ansøgnings publiceringsdag: **2010-10-06**

(86) International ansøgning nr.: **US2008084789**

(87) Internationalt publikationsnr.: **WO2009070639**

(30) Prioritet: **2007-11-28 US 990759 P** **2008-05-29 US 56925 P**

(84) Designerede stater: **AT BE BG CH CY CZ DE DK EE ES FI FR GB GR HR HU IE IS IT LI LT LU LV MC MT NL NO PL PT RO SE SI SK TR**

(73) Patenthaver: **IRX Therapeutics, Inc., 654 Madison Avenue, Suite 1601, New York, NY 10065, USA**

(72) Opfinder: **SIGNORELLI, Kathy, L., 15 Ginger Bread Road, Kings Park, NY 11754, USA**  
**CZYSTOWSKA, Margareta, 5260 Centre Avenue, Apt. 504, Pittsburgh, PA 15232, USA**  
**EGAN, James, E., 2 Cedar Hill Road, Stony Brook, NY 11790, USA**  
**BRANDWEIN, Harvey, 39 Willow Gate, East Hills, NY 11577, USA**  
**WHITESIDE, Theresa, L., 204 Schenley Road, Pittsburgh, PA 15217, USA**  
**HADDEN, John, W., 428 Harbor Road, Cold Spring Harbor, NY 11724, USA**

(74) Fuldmægtig i Danmark: **RWS Group, Europa House, Chiltern Park, Chiltern Hill, Chalfont St Peter, Bucks SL9 9FG, Storbritannien**

(54) Benævnelse: **FREMGANGSMÅDE TIL FORØGELSE AF EN IMMUNOLOGISK VIRKNING**

(56) Fremdragne publikationer:  
**WO-A2-03/035004**  
**US-A1- 2003 206 885**  
**US-A1- 2005 124 645**  
**US-A1- 2007 031 372**  
**US-A1- 2007 065 415**  
**US-A1- 2007 196 335**

**VERASTEGUI E ET AL: "A NATURAL CYTOKINE MIXTURE (IRX-2) AND INTERFERENCE WITH IMMUNE SUPPRESSION INDUCED IMMUNE MOBILIZATION AND REGRESSION OF HEAD AND NECK CANCER", INTERNATIONAL JOURNAL OF IMMUNOPHARMACOLOGY, ELMSFORD, NY, US, vol. 19, no. 11/12, 1 January 1997 (1997-01-01), pages 619-627, XP001205421, ISSN: 0192-0561, DOI: 10.1016/S0192-0561(97)00059-3**  
**BARRERA J L ET AL: "Combination immunotherapy of squamous cell carcinoma of the head and neck", ARCHIVES OF OTOLARYNGOLOGY HEAD AND NECK SURGERY, AMERICAN MEDICAL ASSOCIATION, US, vol. 126, no. 3, 1 March 2000 (2000-03-01) , pages 345-351, XP002967974, ISSN: 0886-4470**

DK/EP 2234642 T3

# DESCRIPTION

## BACKGROUND OF THE INVENTION

### (1) Field of the invention

**[0001]** The present invention relates to therapy of the immune system. In particular, the present invention relates to a primary cell derived biologic and uses thereof.

### (2) Description of related art

**[0002]** In a functioning and competent immune system, immature dendritic cells ingest antigens and migrate to the lymph nodes, where they mature. The resulting mature dendritic cells are then able to activate naïve T cells, creating antigen-specific cytotoxic T cells that then proliferate, enter the circulation, and search out and kill the antigenic target. This is generally a powerful, effective, and fast response. For example, the immune system is able to clear out an influenza infection between 7-12 days.

**[0003]** Antigenic targets can only be eliminated if the immune system is competent. Tumors and various other antigenic targets have effectively evolved strategies to successfully evade the host immune system, and various molecular and cellular mechanisms responsible for tumor evasion have been identified. Some of these mechanisms target immune antitumor effector cells. For example, dysfunction and apoptosis of these cells in the tumor-bearing host creates an immune imbalance that cannot be corrected by immunotherapies aimed only at activation of anti-tumor immune responses.

**[0004]** Apoptosis, or Type I cell death, is a type of programmed cell death and can be induced by stress, infection, or DNA damage. Apoptosis is an integral process during development; however, in certain instances it can actually do harm. For example, apoptosis of lymphocyte/hematopoietic populations, including T cells, can be a serious problem during cancer therapy-related chemotherapy and/or radiation therapy. These cells tend to be sensitive to chemotherapy and radiation therapy.

**[0005]** There are two major mechanisms controlling apoptosis in the cell, the p53 pathway (pro-apoptotic) and the nuclear factor kappa B (NF-κB) pathway (anti-apoptotic). Both pathways are frequently deregulated in tumors, as p53 is usually lost, while NF-κB becomes constitutively active.

**[0006]** Tumor-induced apoptosis of lymphocytes is thought to play a significant role in the immune suppression seen in cancer patients. Apoptosis of anti-tumor effector cells has been

associated with expression of FasL on the surface of tumor cells. This is based on well-documented evidence that Fas/FasL interactions play an important role in the down-modulation of immune functions, including triggering of activation-induced cell death (AICD), to maintain central and peripheral tolerance. Many human tumors express FasL and can eliminate activated Fas+ effector lymphocytes via the Fas/FasL pathway. FasL expression on tumor cells has been shown to negatively correlate with patient prognosis. In addition, it has been shown that tumors can release membrane-associated FasL through secretion of membranous microvesicles (MVs), thereby providing an explanation for spontaneous apoptosis of T lymphocytes observed in the peripheral circulation of patients with cancer.

**[0007]** Applicants previously showed that MV detected in sera of patients with oral carcinoma induced caspase-3 cleavage, DNA-fragmentation, cytochrome c release, loss of mitochondrial membrane potential (MMP) and TCR  $\zeta$ -chain down-regulation in activated T lymphocytes. Furthermore, Applicants demonstrated that these tumor-derived MV are distinguishable from immune cell-derived MV by their unique molecular profile and immune-suppressive properties. Recent data also indicate that MVs are present in sera of patients with squamous cell carcinoma of head and neck (H&NSCC) and that these MVs contain biologically active FasL which may be involved in mediating lysis of Fas positive T cells in the peripheral circulation. Thus, the activity of tumor-derived MV might significantly contribute to the dysfunction and death of effector T cells in cancer patients. The loss of these cells could be responsible for inadequate anti-tumor function and, by extension, inadequate immune responses to cancer vaccines.

**[0008]** It has been convincingly demonstrated that H&NSCC is able to induce functional defects and apoptosis in immune effector cells as well as antigen-presenting cells (APCs) by various mechanisms. In previous studies, Applicants have observed a high level of apoptosis of tumor-infiltrating lymphocytes (TIL) and T lymphocytes in the peripheral circulation of H&NSCC and melanoma patients. Applicants demonstrated that CD8+ T cells are more sensitive to apoptosis than CD4+ cells, and that the effector and tumor-specific subpopulations of CD8+ T cells are preferentially targeted for apoptosis. Also, individuals with HIV generally experience immune suppression caused by dramatic reductions in helper T cell populations. This reduction is caused by apoptosis of the HIV-infected helper T cells.

**[0009]** The mechanisms responsible for immune cell dysfunction in patients with cancer are numerous and varied. In addition to a wide variety of soluble immunosuppressive factors such as PGE2, TGF- $\beta$ , IL-10, and VEGF, and pro-apoptotic ligands such as FasL (described above) that are released by tumor cells or other cells in the tumor microenvironment, suppressor cell populations, i.e., regulatory T cells (T regs), have been shown to play a key role in down-regulation of anti-tumor host immunity.

**[0010]** Collectively, these mechanisms create a poisonous environment, which explains the failure of immunotherapy approaches in the past. In order to have an effective therapeutic outcome, these tumor-induced mechanisms of immune suppression must be directly addressed. With the newfound knowledge of the multiple causes of immune dysfunction seen

in cancer patients, it is becoming more apparent that multiple active components are needed to create an effective cancer immunotherapy. However, there have been many difficulties in finding an effective immunotherapy and understanding its mechanism of action.

**[0011]** Since toxin-induced tumor regressions of human cancer achieved by William Coley early in the 20<sup>th</sup> century, cancer therapists have employed hundreds of different immune therapies with only relatively rare clinical responses. Because there was little or no insight into the cause of these failures, no consistent mechanism of action emerged. In order to establish a clear mechanism of action, a therapy needed to be devised which could consistently produce a response that could then be dissected.

**[0012]** Head and neck squamous cell cancer (H&NSCC) offers a good model since much is known about the immune defects seen in these patients. They include, to name a few, (Whiteside, 2001; Hadden, 1995): 1) T lymphocyte anergy and depletion induced by tumor and host-mediated mechanism including prostaglandins, T regs, myeloid suppressor cells, antigen-antibody complexes, and cytokines such as IL-10; 2) monocyte/macrophage functional defects with evidence of suppressor and inflammatory changes (Mantovani, 2002); and 3) dendritic cell (DC) defects characterized by sinus histiocytosis (SH) (Dunn, 2005).

**[0013]** Effective therapeutic efforts were needed to reverse these multiple defects. An extensive review of the literature (Hadden, 1995) and a series of pre-clinical experiments resulted in the primary cell-derived biologic (also known as IRX-2) protocol. The IRX-2 protocol, shown in FIGURE 1, employs an initial dose of low dose cyclophosphamide (CY) (300 mg/m<sup>2</sup>) by intravenous infusion to reverse suppression by T regs and perhaps other forms of suppressors. The CY is followed by 10-20 daily injections of IRX-2 at the base of the skull to feed into the jugular chains of lymph nodes regional to the cancer.

**[0014]** IRX-2 was originally thought to act via increasing T lymphocyte number and function. Recent evidence indicates that reversal of tumor-induced apoptosis is also a major mechanism, as disclosed in U.S. Provisional Patent Application No. 60/990,759 to Signorelli, et al. Indomethacin (INDO) was administered daily for approximately 21 days to block prostaglandin production by tumor and monocyte/macrophages, a known cancer related suppression mechanism. Zinc was also administered as another aspect of the immunorestorative component of the strategy (Hadden, 1995).

**[0015]** Additionally, at the time the protocol was developed, the critical role played by dendritic cells as presenters of tumor antigen to T cells was unknown. It was also unknown that sinus histiocytosis (SH) reflected a DC defect, and specifically a tumor induced failure of maturation and antigen presentation. Mechanism of action studies disclosed in United States Patent Nos. 6,977,072 and 7,153,499 to Applicants made it clear that the IRX-2 protocol reverses this DC defect and produces changes in regional lymph nodes which reflect a potent immunization (Meneses, 2003). More specifically, these patents disclose a method of inducing the production of naïve T cells and restoring T cell immunity by administration of IRX-2, which preferably includes the cytokines IL-1 $\beta$ , IL-2, IL-6, IL-8, INF- $\gamma$ , and TNF- $\alpha$ . This was one of the first

showings that adult humans can generate naïve T cells through molecular therapy. The presence of naïve T cells available for antigen presentation was important in the restoration of immunity.

**[0016]** The mechanistic hypothesis that underpins IRX-2 is similar to that of a therapeutic cancer vaccine, although no exogenous antigen is required. When administered into the neck, the agent is thought to act in the cervical lymph node chain directly on DCs to promote their maturation and subsequent ability to present endogenous tumor antigen to naïve T cells.

**[0017]** Non-clinical data regarding the mechanism of action of IRX-2 has shown that the agent effectively stimulates and activates human monocyte-derived DCs (Egan, 2007). IRX-2 treatment of immature DCs increased expression of CD83 and CCR7 (markers for maturation and lymph node migration, respectively), as well as differentiation molecules that are important for antigen presentation to naïve T cells. Additionally, IRX-2 induces CD40, CD54, and CD86, which are co-stimulatory receptors that are critical for activation of naïve T cells. Functional changes in IRX-2-treated DCs included an increase in antigen presentation and T cell activity. Taken collectively, IRX-2 treatment of immature DC drives morphologic, phenotypic, and functional changes that are consistent with the development of mature and activated DCs that are able to effectively stimulate naïve T cells.

**[0018]** In contrast to defined antigen-based therapeutic cancer vaccines where antigen-specific reactivity can be measured, rejection antigens have not been discovered in H&NSCC, thus limiting the ability to measure antigen-specific reactivity after IRX-2 therapy.

**[0019]** While IRX-2 was shown to increase T lymphocyte function and generate new immature T cells, there was no disclosure or suggestion and thus no conclusive demonstration that IRX-2 prevented apoptosis of those T cells once generated and it was not known what the function of the T cells were after presentation of antigen. There were no experimental results that showed that apoptosis of T cells was prevented or would even suggest the mechanism of action. Proliferation and apoptosis are separate cellular processes and it would be imprudent to assume that a factor that causes proliferation would necessarily protect from programmed cell death. The exact mechanism by which IRX-2 restores the antitumor response of T cells, and prevents their apoptosis, was neither expressly nor inherently disclosed in the prior art. Furthermore, while IRX-2 was shown to be effective in the mechanisms described above during cancer treatment, there has been no evidence that IRX-2 provides the same mechanism of action in other instances of immune suppression besides cancer.

**[0020]** Not only have individual cytokines not been able to completely restore each part of the immune system through the promotion of DC maturation, the generation of new T cells, and prevention of their apoptosis; but other therapeutics including multiple cytokines have not been able to do this as well. For example, MULTIKINE® (Cel-Sci) is effective only on the tumor itself, affecting the cell cycle of the tumor cells. PROVENGE® (sipuleucel-T, Dendreon), GVAX® (Cell Genesys), PROMUNE® (Coley Pharmaceutical Group), Dynavax TLR 9 ISS, ONCOPHAGE® (vitespen, Antigenics), CANVAXIN® (CancerVax), and TROVAX® (Oxford BioMedica) have

been able to show antigen amplification, dendritic cell processing, and some cellular adjuvancy. TREMELIMUMAB® (Pfizer) and IPILIMUMAB® (Medarex and Bristol-Myers Squibb) only target the T regulatory cell population.

**[0021]** In addition, some therapeutic agents have addressed the issue of apoptosis of cells. There are several biological agents and small molecules that have been developed to prevent cellular and lymphocyte apoptosis. For example, International Patent Application Publication WO/2006/039545 to Maxim Pharmaceuticals, Inc. discloses the administration of a PARP-1 inhibitor and additionally an inhibitor of reactive oxygen metabolite (ROM) production or release to protect tumorcidal lymphocytes, including cytotoxic T lymphocytes and NK cells, from apoptosis. A cytotoxic lymphocyte stimulatory composition including various cytokines can be co-administered. This application reports that free radicals produced by tumor adjacent phagocytes cause dysfunction and apoptosis in tumorcidal or cytotoxic lymphocytes.

**[0022]** International Patent Application Publication WO/2005/056041 to Cleveland Clinic Foundation discloses latent TGF- $\beta$  as a compound that can be used to protect a patient from treatments that induce apoptosis. The latent TGF- $\beta$  induces NF- $\kappa$ B activity, thus preventing apoptosis.

**[0023]** International Patent Application Publication WO/2007/060524 to Fundacion de la Comunidad Valenciana discloses various ringed compounds that are inhibitors of Apaf-1 and therefore act as apoptosis inhibitors. Apaf-1 is an apoptotic protease-activating factor that makes up part of an apoptosome. Caspase-9 is activated within the apoptosome and initiates apoptotic signals.

**[0024]** Amifostine (ETHYOL, MedImmune) is another compound that is administered in order to reduce toxicities resulting from chemotherapy and radiotherapy. More specifically, it is an intravenous organic thiophosphate cytoprotective agent.

**[0025]** There are several disadvantages to these present treatments. For biological agents, there is the problem of difficulty in manufacturing and possible difficulty in specifically targeting a given cell population. For small molecules, there may be a problem of toxicity if used systemically. Further, agents with a single mechanism of action have shown a lack of efficacy because multiple activities are needed to promote anti-apoptotic effects in lymphocyte cell populations. Also, none of these treatments directly address the immunosuppressive environment created by the tumor. Thus, effective adjuvants and approaches to neutralize the tumor-induced suppression are lacking in the prior art.

**[0026]** In essence, the earlier work of Applicants described the mechanism of action of the primary cell derived biologic with respect to DC maturation and generation of naïve T cells, i.e. several specific levels of affecting the immune system. Presented herein is evidence of another level of effect, of the primary cell derived biologic, namely promotion of the survival of lymphocytes. The data herein, taken together with prior disclosures by the Applicants, show that the primary cell derived biologic has a corrective and positive effect on the generation and

activation of specific effectors, and their subsequent survival - each level of the immune system, i.e. each arm of the immune system. Compositions of the prior art are directed to only one of these levels.

**[0027]** Therefore, there is a need for a composition that can effectively enhance both effector generation and effector survival and target each arm of the immune system to restore the immune system and provide a complete mechanism of action against immune suppression.

#### BRIEF SUMMARY OF THE INVENTION

**[0028]** The present invention relates to the use of a natural primary cell-derived biologic comprising interleukin 1 $\beta$  (IL-1 $\beta$ ), interleukin 2 (IL-2), interleukin 6 (IL-6), interleukin 8 (IL-8), tumour necrosis factor  $\alpha$  (TNF- $\alpha$ ) and  $\gamma$ -interferon (IFN- $\gamma$ ), for prolonging the life of T cells *in vitro*.

#### BRIEF DESCRIPTION OF THE SEVERAL VIEWS OF THE DRAWINGS

**[0029]** Other advantages of the present invention will be readily appreciated as the same becomes better understood by reference to the following detailed description when considered in connection with the accompanying drawings wherein:

FIGURE 1 is a display of the IRX-2 protocol;

FIGURE 2 is a representation of the mechanism of action of IRX-2 in combination with a chemical inhibitor and NSAID;

FIGURE 3 is a representation of the mechanism of action of IRX-2;

FIGURE 4A shows CD8+ Jurkat cells analyzed for Annexin V binding by flow cytometry, FIGURE 4B shows Caspase activation detected by FITC-VAD-FMK staining and flow cytometry; FIGURE 4C shows mean percentage +/- standard deviation (SD) of Annexin V-positive/7-AAD-negative Jurkat cells following incubation with various apoptosis-inducing agents, and FIGURE 4D shows mean percentage +/- SD of FITC-VAD-FMK+ Jurkat T cells following incubation with various apoptosis-inducing agents;

FIGURE 5A shows a time-course analysis of CD8+ Jurkat cells, and FIGURE 5B shows a concentration-course analysis;

FIGURE 6 shows a graph of percentage of FITC-VAD-FMK positive cells for various treatments of CD8+ Jurkat cells;

FIGURE 7 is a graph of Caspase-activation in Jurkat CD8+ cells after treatment with IRX-2 or cytokines and incubation with tumor-microvesicles (MV);

FIGURE 8A is a graph of human peripheral blood pre-activated CD4+ cells and FIGURE 8B is a graph of human peripheral blood pre -activated CD8+ cells treated with tumor-MV (15 µg) and pre-treated with the indicated cytokines or IRX-2;

FIGURE 9A is a graph of activated human peripheral blood pre-activated CD4+ cells and FIGURE 9B is a graph of human peripheral blood pre-activated CD8+ cells treated with CH-11 Ab (400 ng/mL) following pre-treatment with the indicated cytokines or IRX-2;

FIGURE 10A shows activation of caspases-3 and 7 in CD8+ Jurkat cells assessed via flow cytometry for caspase 3/7-FAM binding, and FIGURE 10B shows Western immunoblots showing caspase-3 activation in CD8+ Jurkat cells;

FIGURE 11A shows CD8+ Jurkat cells were analyzed by flow cytometry for a decrease in red fluorescence of the cationic dye JC-1, indicating a loss of MMP, and FIGURE 11B is a graph of percentage of JC-1 red-negative cells;

FIGURE 12A is a fluorescent microscopy of CD8+ Jurkat cells which were either untreated (a), incubated for 24 hours with IRX-2 alone (b) or MV alone for 24 hours (c) or pre-incubated with IRX-2 for 24 hours and subsequently treated with MV for 24 hours (d) and then stained by the TUNEL method to reveal DNA strand breaks (red nuclei) indicative of apoptosis, and FIGURE 15B is a graph of percentage of TUNEL-positive CD8+ Jurkat cells in the above co-cultures;

FIGURE 13 shows Western blots of CD8+ Jurkat cells with various treatments;

FIGURE 14A is a graph showing that pretreatment of cells with IRX-2 reverses the MV-induced changes in the ratios of pro- and anti- apoptotic proteins, and FIGURE 14B is a representative dot plot and corresponding histogram showing that IRX-2 treatment modulates the expression of pro- and anti-apoptotic proteins;

FIGURE 15A is a Western blot of CD8+ Jurkat cells with various treatments, and FIGURE 15B is a graph of percentage of FITC-VAD-FMK positive cells;

FIGURE 16 is a graph of *in vivo* dose response for IRX-2;

FIGURE 17 is a graph of percentage of survival in four groups of patients;

FIGURE 18 is a graph of median percentage of lymphocyte infiltration in four groups of patients;

FIGURE 19 is a photograph of H&E staining for lymphocytes;

FIGURE 20 is a photograph of H&E staining for lymphocyte infiltration;

FIGURE 21 is a graph of lymphoid infiltration density in responders, and FIGURE 26B is a graph of lymphoid infiltration density in non-responders;

FIGURE 22 is a graph of location of intratumoral/peritumoral lymphocyte infiltrates;

FIGURE 23 is a photograph of IHC staining for CD45RO+ memory T cells;

FIGURE 24 is a photograph of fused FDG PET/CT scan images at day 0 and day 21;

FIGURE 26 is a graph of overall survival for Stage IVa patients;

FIGURE 27A is a graph of node size, FIGURE 27B is a graph of T cell area, FIGURE 27C is a graph of sinus histiocytosis, and FIGURE 27D is a graph of T cell density as compared in controls, H&NSCC controls, and H&NSCC patients administered IRX-2;

FIGURES 28A is a photograph of H&E staining of a typical lymph node in a head and neck cancer patient with sinus histiocytosis, Figure 28B is a photograph of H&E and CD68 staining of a typical lymph node in a head and neck cancer patient with sinus histiocytosis, Figure 28C is a photograph of H&E staining of a lymph node with erythrocyte congestion in a head and neck cancer patient with sinus histiocytosis, and Figure 28D is graph showing that IRX-2 treatment increases the number of activated dendritic cells in lymph nodes;

FIGURES 29A-Care photographs of H&E staining of tumor samples of patients with head and neck cancer showing a lack of lymphocyte infiltration;

FIGURES 29D-F are photographs of H&E staining of tumor samples of patients with head and neck cancer after IRX-2 treatment showing a lack of lymphocyte infiltration;

FIGURE 30 is a graph of fibrosis and necrosis in responders and non-responders;

FIGURE 31A is a photograph of tumor fragmentation, FIGURE 31B is a photograph of lymphocyte infiltration, and FIGURES 31C-D are photographs of killer T cells;

FIGURE 32 is a display of the mechanism of IRX-2 restoring dendritic cell function by up-regulating key activation receptors;

FIGURE 33A is a graph of antigen presentation increase (HLA-DR) by IRX-2, and FIGURE 33B is a graph of co-stimulation increase (CD86) by IRX-2;

FIGURE 34A is a graph of up-regulation of CD40 by IRX-2, and FIGURE 34B is a graph of up-regulation of CD54 by IRX-2;

FIGURE 35 is a graph of CD83 expression with IRX-2;

FIGURE 36 is a graph of dendritic cell -mediatedT cell stimulationafter IRX-2 treatment;

FIGURE 37A is a graph of delayed type hypersensitivity and FIGURE 37B is a graph of increase in IFN- $\gamma$  with IRX-2;

FIGURE 38 is a graph of delayed type hypersensitivity compared across treatments;

FIGURE 39 is a display of evidence of action on immune cells in peripheral circulation;

FIGURE 40 is a graph of T reg counts with IRX-2 treatment; and

FIGURE 41A is an image of a tumor pre-treatment with IRX-2, and FIGURE 46B is an image of

a tumor post-treatment with IRX-2.

## DETAILED DESCRIPTION OF THE INVENTION

**[0030]** In general, the present invention is directed to the application of the mechanism of action of a natural primary cell-derived biologic IRX-2 with respect to prolonging the life of lymphocytes *in vitro*.

### Definitions

**[0031]** As used herein, the term "immune target" refers to any antigenic source or entity that can be rendered antigenic and afflicts the host patient. Generally, such targets, such as immunogenic pathogens and tumors, show surface antigen that would otherwise induce an immune response in an immune competent patient. In addition, exogenous antigen can cause an otherwise non-immunogenic immune target to be susceptible to immune attack in an immune competent patient. With specific regard to the present invention, the immune target is immunogenic or potentially immunogenic to which the immune system is nonresponsive due to immune incompetence from any cause. In the present invention, the immune target is "targeted" by the immune system made competent by the primary cell derived biologic which reverses the immune suppression and restores the immune system to function.

**[0032]** The immune incompetence can be caused by genetic defects in the components of the immune system (intrinsic, or primary immune deficiencies). The immune suppression can also be caused by extrinsic factors (secondary immune deficiencies). For example, diseases such as AIDS or HIV, irradiation (radiotherapy), chemotherapy, malnutrition, burns, infections, and cancer (tumors) can cause immune suppression.

**[0033]** As used herein, "apoptosis" refers to cell death. As stated above, apoptosis (Type I cell-death) is a type of programmed cell death that occurs for various reasons such as stress, infection, or DNA damage. Apoptosis of lymphocytes can be induced by a variety of phenomena, such as, but not limited to cancer-related therapies (chemotherapy, radiation), and tumors themselves producing apoptosis-inducing factors.

**[0034]** As used herein, "effective amount" refers to an amount of primary cell derived biologic that is needed to achieve the desired result of the present invention, namely, protecting lymphocytes and other hematopoietic components from apoptosis as well as activating the immune system to attack an immune target. One skilled in the art can determine the effective amount of the primary cell derived biologic that should be given to a particular patient.

**[0035]** As used herein, "increasing immunological effect" refers to the process of changing an

incompetent immune system to a competent immune system. The function of a single component of the immune system is reversed from incompetent to competent, and preferably, the function of multiple components is reversed from incompetent to competent. Therefore, the effect that the immune system has on an immune target is increased. A competent immune system is required to effectively destroy tumors and other immune targets. Not merely turning on but preventing breakdown so that there is a build up of immunity.

**[0036]** As used herein, "lymphocytes" refers to a white blood cell present in the immune system and includes large granular lymphocytes (natural killer (NK) cells) and small lymphocytes (T cells and B cells).

**[0037]** A "primary cell derived biologic", as used herein, is a combination of cytokines, preferably natural and non-recombinant cytokines, also previously known as a natural cytokine mixture (NCM). Preferably, the primary cell derived biologic is IRX-2 (citoplurikin) as described below, and the two terms can be used interchangeably throughout this application without deviation from the intended meaning.

**[0038]** "IRX-2", also known as "citoplurikin", is a leukocyte-derived, natural primary cell derived biologic produced by purified human white blood cells (mononuclear cells) stimulated by phytohemagglutinin (PHA) and ciprofloxacin (CIPRO). The major active components are interleukin 1 $\beta$  (IL-1 $\beta$ ), interleukin 2 (IL-2), interleukin 6 (IL-6), interleukin 8 (IL-8), tumor necrosis factor  $\alpha$  (TNF- $\alpha$ ), and  $\gamma$ -interferon (IFN- $\gamma$ ). Preferably, the IRX-2 used in the present invention includes these six critical cytokines. IRX-2 has also previously been referred to as an "NCM", a natural cytokine mixture, defined and set forth in United States Patent Nos. 6,977,072 and 7,153,499.

**[0039]** Briefly, IRX-2 is prepared in the continuous presence of a 4-aminoquinolone antibiotic and with the continuous or pulsed presence of a mitogen, which in the preferred embodiment is PHA. Other mitogens, however, can also be used. The IRX-2 produced for administration to patients contains a concentration of IL-1 $\beta$  that ranges from 60 - 6,000 pcg/mL, more preferably, from 150 - 1,800 pcg/mL; a concentration of IL-2 that ranges from 600-60,000 pcg/mL, more preferably, from 3,000-12,000 pcg/mL, and concentrations of IFN- $\gamma$  and TNF- $\alpha$  that range from 200-20,000 pcg/mL, more preferably, from 1,000-4,000 pcg/mL.

**[0040]** IRX-2 can also contain a concentration of IL-6 that ranges from 60-6,000 pcg/mL, more preferably, from 300-2,000 pcg/mL; a concentration of IL-8 that ranges from 6,000-600,000 pcg/mL, more preferably from 20,000-180,000 pcg/mL; a concentration of TNF- $\alpha$  that ranges from 200-20,000 pcg/ml, more preferably, from 1,000-4,000 pcg/mL. Recombinant, natural or pegylated cytokines can be used, or IRX-2 can include a mixture of recombinant, natural or pegylated cytokines. The IRX-2 of the present invention can further include other recombinant, natural or pegylated cytokines such as IL-7, IL-12, IL-15, GM-CSF (at a concentration that ranges from 100-10,000 pcg/mL, more preferably from 500-2,000 pcg/mL), and G-CSF. The method of making IRX-2 is disclosed in the above cited patents as well as in

U.S. Provisional Patent Application No. 61/044,674.

**[0041]** "Tumor escape" as used herein refers to any mechanism by which tumors escape the host's immune system.

### **The Overall Mechanism of the Primary Cell Derived Biologic**

**[0042]** The present invention is directed to the use of the primary cell-derived biologic comprising interleukin 1 $\beta$  (IL-1 $\beta$ ), interleukin 2 (IL-2), interleukin 6 (IL-6), interleukin 8 (IL-8), tumour necrosis factor  $\alpha$  (TNF- $\alpha$ ) and  $\gamma$ -interferon (IFN-  $\gamma$ ) for prolonging the life of lymphocytes *in vitro*.

### **Blocking Immune Destruction**

**[0043]** Immune destruction is blocked by protecting the activated T cells from apoptosis. One of the mechanisms of tumor escape involves targeted elimination of CD8+ effector T cells through apoptosis mediated by tumor-derived microvesicles (MV). Immunosuppressive MV have been found in neoplastic lesions, sera, ascites and pleural effusions obtained from cancer patients and have been linked to apoptosis and TCR alterations in effector T cells in these patients. MV-driven elimination of effector T cells, which are necessary for anti-tumor host defense, contributes to tumor escape and cancer progression. Therefore, protection of anti-tumor effector cells from functional impairments and death is a major objective of immune therapy. Clinical and experimental data show that certain cytokines, especially survival cytokines using the common receptor  $\gamma$  chain, are able to protect activated T cells from tumor-induced death and enhance their anti-tumor activity.

**[0044]** More specifically, there are several ways in which IRX-2 protects T cells from apoptosis. The expression of anti-apoptotic signaling molecules (i.e. JAK-3 and phosphor-Akt) is up-regulated and the expression of pro-apoptotic molecules (i.e. SOCS-2) is down-regulated. Activation of caspases in CD8+ and CD4+ T lymphocytes is decreased and cFLIP expression is increased. Inhibition of the PI3K/Akt survival pathway is counteracted by IRX-2. The T cells are protected from both extrinsic apoptosis (MV-induced and FasL-induced apoptosis) and intrinsic metabolic (cellular stress or DNA damage related) apoptosis.

**[0045]** The protection from extrinsic MV-induced apoptosis is further accomplished by preventing down-regulation of JAK3, CD3- $\zeta$ , and STAT5; inhibiting dephosphorylation of Akt-1/2; and maintaining balanced ratios of Bax/Bcl-2, Bax-Bcl-xL, and Bim/Mcl-1. The protection from MV-induced apoptosis is also accomplished by preventing induction of the activity of caspase-3 and caspase-7. More specifically, the induction of the active cleaved form of caspase-3 is blocked, as is the loss of mitochondrial membrane potential. Nuclear DNA fragmentation is inhibited. Protection from intrinsic apoptosis by IRX-2 is shown by its

protection of activated T cells from staurosporine-induced apoptosis.

**[0046]** Importantly, the cytokines of IRX-2 protect the activated T cells from apoptosis in a synergistic manner. In other words, the combination of the cytokines in IRX-2 produces a greater affect than is seen by administering individual cytokines alone.

**[0047]** The primary cell derived biologic, i.e. IRX-2, administered is preferably as described above. A chemical inhibitor, low dose cyclophosphamide is preferably administered prior to administering the IRX-2, which reverses suppression by Tregs lymphocytes. An NSAID (preferably indomethacin) and zinc can also be administered daily during the IRX-2 regimen. Dosing of IRX-2 is further described below.

#### Other Embodiments

**[0048]** The present invention provides for a method of protecting activated T cells from apoptosis, including the steps of administering an effective amount of a primary cell derived biologic (IRX-2), and protecting activated T cells from apoptosis. Essentially, the method of protecting activated T cells from apoptosis enhances their anti-tumor activity, because the T cells live longer to perform their necessary functions.

**[0049]** The present invention also provides for a method of enhancing the anti-tumor activity of T cells, including the steps of administering an effective amount of a primary cell derived biologic, stimulating the production of naïve T cells, activating the naïve T cells, protecting the activated T cells from apoptosis, and enhancing the anti-tumor activity of the T cells. Naïve T cells are produced in response to the administration of IRX-2, as disclosed in U.S. Patent Nos. 6,977,072 and 7,153,499. These naïve T cells become activated and mature through the presentation of tumor antigen. According to the present invention, the IRX-2 can now protect these activated T cells from apoptosis. This protection is accomplished as described above.

**[0050]** The present invention also provides for a method of prolonging the life of lymphocytes, including the steps of administering an effective amount of a primary cell derived biologic (IRX-2), and prolonging the life of lymphocytes. The lymphocytes that are affected by IRX-2 are preferably T cells. IRX-2 can further prolong the life of other cells that could be affected by apoptosis, such as B cells and hematopoietic populations, (dendritic cells, monocytes and myeloid cells). IRX-2 prevents the T cells from otherwise dying, thus prolonging their lives and allowing them to acquire and exert the anti-tumor effects for which they are programmed, e.g. cytolytic activity or T helper activity. In other words, the IRX-2 prevents apoptosis of the T cells, thus prolonging the lives of the T cells.

**[0051]** There are several advantages of the present invention with regard to apoptosis. First, the primary cell derived biologic used in the present invention is a well-defined biologic that is manufactured in a robust and consistent manner (IRX-2). This is unlike the previously disclosed prior art compounds that are able to protect T cells from apoptosis, but are not

manufactured robustly. Further, the cytokines in the primary cell derived biologic used in the present invention act synergistically on multiple cell types of the immune system resulting in a coordinated immune response at doses far lower than are needed to achieve similar results using single, recombinant cytokines as monotherapies, as evidenced in the examples below.

**[0052]** As shown in the following examples, it was determined that IRX-2 is able to protect T cells from apoptosis mediated by tumor-derived MV. Some of the cytokines present in the IRX-2 such as IL-2 are known to have anti-apoptotic effects; thus, it was reasonable to evaluate whether the IRX-2 had protective as well as stimulatory effects on T cells. The combined effects of T cell survival enhancement and functional stimulation underlie IRX-2's apparent synergistic effects *in vivo*. Using a previously established *in vitro* model of tumor-induced apoptosis, it is demonstrated herein that IRX-2 provides strong protection to T cells from apoptosis mediated by tumor-derived MV through activation of survival pathways, thereby effectively counteracting cancer-related immunosuppression. The results of these experiments are presented in the examples below. Thus, it is shown herein that IRX-2 is effective against a new arm of the immune system and is able to restore that arm of the immune system, i.e. preventing apoptosis of lymphocytes.

**[0053]** Tumor-derived microvesicles (MV) expressing a membrane form of FasL were purified from supernatants of the PCI-13 tumor cell line and co-incubated with CD8+ Jurkat cells or activated peripheral blood (PB) T cells. FasL, the Fas ligand, is a type II transmembrane protein belonging to the tumor necrosis factor (TNF) family. FasL-receptor interactions play an important role in the regulation of the immune system and the progression of cancer. Apoptosis is induced upon binding and trimerization of FasL with its receptor (FasR), which spans the membrane of a cell targeted for death.

**[0054]** Incubation of CD8+ Jurkat T cells and activated PB T cells with tumor-derived MV induced significant apoptosis, as evidenced by increased annexin binding (64.4 %  $\pm$  6.4), caspase activation (58.1 %  $\pm$  7.6), a loss of mitochondrial membrane potential (MMP) (82.9 %  $\pm$  3.9) and DNA-fragmentation.

**[0055]** Pre-incubation of T cells with IRX-2 suppressed apoptosis in a dose- and time-dependent manner ( $p < 0.001$  to  $p < 0.005$ ). The observed protective effects on CD8<sup>+</sup> T cells of IRX-2 were comparable to the cytoprotective effects of recombinant IL-2 or IL-15 alone but was superior to IL-7; however, IRX-2 had greater effects on protecting CD4<sup>+</sup> T cells from apoptosis. IRX-2 does not contain IL-7 or IL-15 and the fact that it is protecting CD4<sup>+</sup> T cells from apoptosis more effectively than equivalent amounts of recombinant IL-2 means that the unique components of IRX-2 act synergistically to protect T cells from apoptosis.

**[0056]** IRX-2 suppressed MV-induced down-regulation of JAK3 and the TCR-associated  $\zeta$ -chain and induced strong Stat5 activation in T cells. Flow cytometry analysis showed that IRX-2 reversed the MV-induced imbalance of pro- and anti-apoptotic proteins in T cells by suppressing the MV-mediated up-regulation of pro-apoptotic proteins Bax and Bim ( $p < 0.005$

to  $p < 0.05$ ), and concurrently restoring the expression of the anti-apoptotic proteins Bcl-2, Bcl-xL, FLIP and Mcl-1 ( $p < 0.005$  to  $p < 0.01$ ). In addition, IRX-2 treatment counteracted the MV-induced inhibition of the PI3K/Akt survival pathway. A specific Akt-inhibitor (Akti-1/2) abrogated the protective effect of IRX-2, demonstrating that the PI3K/Akt pathway plays a key role in IRX-2-mediated survival signaling. The PI3K/Akt pathway is a key component in preventing apoptosis and activation of this pathway would prevent against many different inducers of apoptosis. These studies show that a short *ex vivo* pre-treatment with IRX-2 provides potent protection of T cells from tumor-induced apoptosis. As effector T cells resistant to immunosuppressive influences of the tumor microenvironment are essential for anti-tumor host defense, utilization of IRX-2 significantly improves the effectiveness of cancer biotherapies.

#### **Advantages of the Primary Cell Derived Biologic**

**[0057]** Overall, IRX-2 unsuppresses and potentiates all aspects of the cellular and humoral arms of the immune system to attack various immune targets. Any immune incompetent disease state (cancer, AIDS, and others as previously described above) can now be reversed by unsuppressing and potentiating the immune system through IRX-2. IRX-2 functions as a "symphony" rather than just a single "instrument" in that the specific combination of cytokines of IRX-2 effect multiple parts of the immune system, as opposed to prior art therapeutics which, while being combinations of components, either augment generation of effectors or prevent their apoptosis, i.e. only work on a single part of the immune system. Each part of the immune system is a gatekeeper of one effect experienced by IRX-2 administration. Each of these parts of the immune system is required in order to attack an immune target. FIGURES 2 and 3 depict the processes potentiated by IRX-2 therapy. Immature dendritic cells must become mature in order to activate naïve T cells. Production of naïve T cells also must be induced so that they can be presented with antigen by the mature dendritic cells. Both the naïve T cells and the dendritic cells must migrate to the regional lymph node in order for antigen to be presented to the naïve T cells by the dendritic cells. Once activated, the T cells must be protected from apoptosis so that they can differentiate into killer T cells and attack the immune target. B cells also mature into plasma cells to aid in attacking the immune target. Administration of IRX-2 augments all of these processes, providing a competent immune system that is ready to attack any immune target.

#### **Dosing and Administration**

**[0058]** As shown below, IRX-2 inhibits apoptosis over a range of concentrations: from 1:1 to 1:10 dilution of the IRX-2 liquid (i.e. dilution of the IRX-2 in the media in which it was produced). The compounds of the present invention (including IRX-2) are administered and dosed to promote protection from apoptosis. The pharmaceutically "effective amount" for purposes herein is thus determined by such considerations as are known in the art. It should be noted that the compounds can be administered as the compounds themselves or as a

pharmaceutically acceptable derivative and can be administered alone or as an active ingredient in combination with pharmaceutically acceptable carriers, diluents, adjuvants and vehicles. The data presented shows activity of the IRX-2 on cells derived from humans, and therefore the data herein is all directly relevant and applicable to humans. The pharmaceutically acceptable carriers, diluents, adjuvants and vehicles as well as implant carriers generally refer to inert, non-toxic solid or liquid fillers, diluents or encapsulating material not reacting with the active ingredients of the invention. The carrier can be a solvent or dispersing medium containing, for example, water, ethanol, polyol (for example, glycerol, propylene glycol, liquid polyethylene glycol, and the like), suitable mixtures thereof, and vegetable oils. Proper fluidity can be maintained, for example, by the use of a coating such as lecithin, by the maintenance of the required particle size in the case of dispersion and by the use of surfactants. Nonaqueous vehicles such as cottonseed oil, sesame oil, olive oil, soybean oil, corn oil, sunflower oil, or peanut oil and esters, such as isopropyl myristate, can also be used as solvent systems for compound compositions. Additionally, various additives which enhance the stability, sterility, and isotonicity of the compositions, including antimicrobial preservatives, antioxidants, chelating agents, and buffers, can be added. Prevention of the action of microorganisms can be ensured by various antibacterial and antifungal agents, for example, parabens, chlorobutanol, phenol, sorbic acid, and the like. In many cases, it is desirable to include isotonic agents, for example, sugars, sodium chloride, and the like.

**[0059]** The invention is further described in detail by reference to the following experimental examples. These examples are provided for the purpose of illustration only, and are not intended to be limiting unless otherwise specified. Thus, the present invention should in no way be construed as being limited to the following examples, but rather, be construed to encompass any and all variations which become evident as a result of the teaching provided herein.

## EXAMPLES

### Materials and Methods

**[0060]** All steps relating to cell culture are performed under sterile conditions. General methods of cellular immunology not described herein are performed as described in general references for cellular immunology techniques such as Mishell and Shiigi (Selected Methods in Cellular Immunology, 1981) and are well known to those of skill in the art.

#### **Antibodies and reagents:**

**[0061]** The following monoclonal antibodies were used for flow cytometry analysis: anti-CD3-ECD, -CD8-PC5, -CD4-PE (Beckman Coulter, Miami, FL); anti-Bcl-2-FITC, -Bcl-2-PE, -Fas-

FITC, -FasL-PE (BD Biosciences, San Jose, CA); anti-Bax-FITC, -Bcl-xL-FITC (Santa Cruz Biotechnology, Santa Cruz, CA) and anti-Bid-antibody (Abcam Inc., Cambridge, MA). Polyclonal antibodies were: anti-Bim (Cell Signaling, Danvers, MA), anti- FLIP (GenWay Biotech, San Diego, CA), and anti- Mcl-1 (Santa Cruz Biotechnology). FITC-conjugated Annexin V was purchased from Beckman Coulter. FITC-conjugated anti-rabbit IgG was purchased from Jackson ImmunoResearch Laboratories (West Grove, PA) and the isotype controls (IgG<sub>1</sub>-FITC, IgG<sub>2a</sub>-FITC and IgG<sub>2b</sub>-FITC and IgG2-PE) were purchased from BD Biosciences. Antibodies purchased for Western Blot analysis included: polyclonal phospho-Akt (Ser473), polyclonal total-Akt, monoclonal phospho-STAT5 (Tyr694) and monoclonal total-STAT5 (Cell Signaling), monoclonal Bcl-2, monoclonal CD3- $\zeta$ , monoclonal JAK3, polyclonal SOCS-2 and polyclonal Mcl-1 (Santa Cruz Biotechnology), polyclonal caspase-3, polyclonal FasL antibody-3 (BD Biosciences) and monoclonal  $\beta$ -actin (Sigma Aldrich, St. Louis, MO). Anti-Fas (CH-11) agonistic monoclonal antibody, IgM isotype control for CH-11, anti-Fas blocking monoclonal antibody, clone ZB4, and isotype IgG1 control for ZB4 were all purchased from Upstate Biotechnology (Lake Placid, NY). All cell culture reagents including AIM V medium, RPMI 1640 medium, phosphate-buffered saline (PBS), heat-inactivated fetal calf serum ( $\Delta$ FCs), streptomycin, penicillin, L-glutamine, recombinant trypsin-like enzyme (TrypLE) and trypan blue dye were purchased from Gibco/Invitrogen (Grand Island, NY). The human recombinant cytokines, rhIL-2, rhIL-7 and rhIL-15, were purchased from Peprotech Inc. (Rocky Hill, NJ). Bovine serum albumin (BSA), saponin, etoposide and staurosporine were from Sigma Aldrich. 7-amino-actinomycin D (7AAD) and the pan caspase inhibitor, z-VAD-FMK, were obtained from BD Biosciences. The selective inhibitor of Akt1/Akt2 was purchased from Calbiochem (San Diego, CA) and the selective inhibitors for caspase-3, caspase-8 and caspase-9 from R&D Systems (Minneapolis, MN).

#### **Preparation of Primary Cell Derived Biologic (IRX-2):**

**[0062]** The method of making the primary cell derived biologic is generally described in U.S. Provisional Patent Application No. 61/044,674. Mononuclear cells (MNCs) are purified to remove contaminating cells by loading leukocytes onto lymphocyte separation medium (LSM) and centrifuging the medium to obtain purified MNCs with an automated cell processing and washing system. The MNCs are then stored overnight in a FEP lymphocyte storage bag. An induction mixture of the MNCs is stimulated with a mitogen, preferably phytohemagglutinin (PHA), and ciprofloxacin in a disposable cell culture device and a primary cell derived biologic is produced from the MNCs. The mitogen is removed from the induction mixture by filtering and tangential flow filtration mode, and then the induction mixture is incubated. The induction mixture is clarified by filtering to obtain a primary cell derived biologic supernatant. Finally, the primary cell derived biologic supernatant is cleared from DNA and adventitious agents by applying anion exchange chromatography and 15 nanometer filtration and optionally further inactivation by ultraviolet-C (UVC). The final product can then be vialled and stored for future administration to a patient.

#### **Cells and cell lines:**

**[0063]** The head and neck squamous cell carcinoma (H&NSCC) cell line PC-13 was established in Applicants' laboratory and maintained as previously described. It was retrovirally transfected with the human FasL gene obtained from Dr. S. Nagata (Osaka Biosciences Institute, Osaka, Japan) as previously reported. Supernatants of transfected PCI-13-cells (PCI-13-FasL), which contained both sFasL and the 42 kDa membranous form of FasL, were used as a source of tumor-derived microvesicles (MV). Jurkat cells were obtained from American Tissue Culture Collection (ATCC, Manassas, VA) and were transfected with CD8. The CD8+ Jurkat cells were cultured in RPMI 1640 medium supplemented with 10% (v/v) fetal bovine serum (FBS), L-glutamine and antibiotics. Human T lymphocytes were isolated from peripheral blood mononuclear cells (PBMC) obtained from consented normal donors. PBMC were isolated by Ficoll-Hypaque density gradient centrifugation (GE Healthcare Bio-Sciences Corp., Piscataway, NJ), washed and plated for 1 hour at 37°C in culture flasks (T162) in an atmosphere of 5% CO<sub>2</sub> to remove CD14+ monocytes. The non-adherent T-lymphocyte fraction was collected and immediately used for experiments or cryopreserved. CD8+ T cells or CD4+ T cells were purified by positive selection using CD8 MicroBeads or CD4 MicroBeads, respectively (Miltenyi Biotec, Auburn, CA) using the AutoMACS system according to the manufacturer's instructions. Purified CD8+ or CD4+ T cells were then cultured for 2-3 days in AIM V medium supplemented with 10% FBS in the presence of beads coated with anti-CD3 and anti-CD28 antibodies (T Cell Activation/ Expansion Kit, Miltenyi Biotec). All cells used for the above described experiments were in the log phase of growth.

#### **Isolation of microvesicles:**

**[0064]** Microvesicles (MV) were isolated from culture supernatants of the FasL-transfected PCI-13 cell line as previously described. Briefly, the concentrated cell culture supernatants were fractioned by a two-step procedure, including size exclusion chromatography and ultracentrifugation. PCI-13-FasL supernatants were concentrated at least 10 times using Centriprep Filters (Fisher Scientific, Pittsburgh, PA). Next, 10 mL aliquots of concentrated supernatants were applied to a Sepharose 2B (Amersham Biosciences, Piscataway, NJ) column (1.5x35 cm) equilibrated with PBS. One milliliter fractions were collected and the protein content was monitored by measuring absorbance at 280 nm. The exclusion peak material, containing proteins of >50 million kDa, was then centrifuged at 105,000 x g for 2 hours at 4°C. The pellet was resuspended in 300-500 µl of sterile PBS. Protein concentration in each MV preparation was estimated by a Lowry's protein assay (Bio-Rad Laboratories, Hercules, CA) with bovine serum albumin (BSA) used as a standard.

#### **Western blot assays:**

**[0065]** To determine total or phosphorylated forms of Akt, Bcl-2, CD3 $\zeta$ , caspase-3, JAK3,

STAT5, FLIP, and Mcl-1, Jurkat CD8+ cells or purified activated CD8+ or CD4+ T-cells were co-incubated with MV at the indicated concentration and/or with IRX-2 (1:3 final dilution) for the indicated period of time at 37°C. The cells were then washed, centrifuged at 4°C and lysed in equal volumes of ice-cold lysis-buffer (50 mM Tris-HCl pH 7.5, 150 mM NaCl, 0.5 % Nonidet P-40) and protease inhibitor cocktail (Pierce Chemical Co., Rockford, IL). After lysis, the homogenates were clarified by centrifugation. The supernatants were isolated, and boiled for 5 minutes in 5x Laemmli sample buffer. Proteins were separated by sodium dodecyl sulfate-polyacrylamide gel electrophoresis (SDS-PAGE) and electrotransferred to polyvinylidene difluoride (PVDF) membranes. The membranes were blocked in 5% fat-free milk or 5% BSA in TTBS (0.05% Tween 20 in Tris-buffered saline) for 1 hour at room temperature (RT) and then incubated overnight at 4°C with the appropriate antibodies. After washing (3x15 minutes) with TTBS at RT, membranes were incubated with horseradish peroxidase-conjugated secondary antibody at 1:150,000 dilution (Pierce Chemical Co) for 1 hour at RT. After washes, membranes were developed with a SuperSignal chemoluminescent detection system (Pierce Chemical Co). To reprobe with another primary antibody, membranes were incubated in stripping buffer (0.5 M NaCl, 3% (v/v) glacial acetic acid), washed and then used for further study.

**Co-incubation of CD8+ Jurkat cells or activated normal T-lymphocytes with MV and IRX-2:**

**[0066]** CD8+ Jurkat cells or activated normal T lymphocytes were plated at  $0.3 \times 10^6$  cells per well in a 96-well plate and pre-treated or not with IRX-2 or with recombinant human cytokines at a final concentration of 10 ng/mL or 100 IU/mL for 24 hours (unless otherwise noted). MV (10 µg protein per  $0.3 \times 10^6$  cells) were then added for 3-24 hours. In some experiments, cells were first co-incubated with MV for 3-24 hours, then washed and treated further with IRX-2 or cytokines or treated for the indicated time period with MV and IRX-2 added simultaneously. In selected blocking experiments, anti-Fas neutralizing monoclonal antibody, ZB-4, the pan-caspase inhibitor, Z-VAD-FMK, or the specific Akt-inhibitor or specific inhibitors for caspase-3, caspase-8 and caspase-9 were added at the indicated concentrations prior to MV co-incubation.

**Cell surface staining:**

**[0067]** MV and/or IRX-2 co-incubated CD8+ Jurkat cells or activated T-lymphocytes (at least 300,000 cells/tube) were washed twice in staining buffer (0.1% w/v BSA and 0.1% w/v NaN<sub>3</sub>). Cells were stained for cell surface markers as previously described. Briefly, cells were incubated with the optimal dilution of each antibody for 20 minutes at RT in the dark, washed twice with staining buffer and finally fixed in 1% (v/v) paraformaldehyde (PFA) in PBS. The following antibodies were used for surface staining: anti-CD3-ECD, anti-CD4-PE, anti-CD8-PC5, anti-Fas-FITC and anti-FasL-PE.

**Flow cytometry:**

**[0068]** Four color flow cytometry was performed using a FACScan flow cytometer (Beckman Coulter) equipped with Expo32 software (Beckman Coulter). Lymphocytes were gated based on morphology, and debris, MV as well as monocytes and granulocytes were excluded, collecting data on at least  $10^5$  cells. For the analysis of activated primary T lymphocytes, gates were restricted to the CD3 $^+$ CD8 $^+$  or CD3 $^+$ CD4 $^+$  T-cell subsets. Data was analyzed using Coulter EXPO 32vl.2 analysis software.

**Annexin V binding assay:**

**[0069]** Annexin V (ANX) binding to MV and/or IRX-2 co-incubated CD8 $^+$  Jurkat cells or activated T lymphocytes was measured by flow cytometry to evaluate spontaneous or *in vitro* induced apoptosis. Following surface-staining with antibodies to CD3, CD8 or CD4, the cells were resuspended in Annexin-binding buffer and incubated with FITC-conjugated Annexin V for 15 minutes on ice. Additional staining with 7-amino-actinomycin D (7-AAD) was performed to discriminate dead and live cells. The cells were analyzed by flow cytometry within 30 minutes of staining.

**Measurement of caspase activation:**

**[0070]** Total cellular Caspase activity was tested by intracellular staining of activated caspases using a pan caspase inhibitor, CASPACE FITC-VAD-FMK In Situ Marker (Promega, Madison, WI). Cells were resuspended in PBS and FITC-VAD-FMK was added at a final concentration of 5  $\mu$ M. The cells were incubated for 20 minutes at 37°C, 5% CO<sub>2</sub> and washed with PBS. Then cells were stained for cell surface receptors, fixed with 1 % paraformaldehyde and analyzed by flow cytometry. The specific activation of caspase-3 and caspase-7 was measured using the VYBRANT FAM caspase-3 and -7 Assay Kit from Invitrogen (Carlsbad, CA) according to the manufacturers' instructions. Briefly, cells were resuspended in PBS and stained with a 150x dilution of the carboxyfluorescein (FAM)-labeled FMK-caspase inhibitor for 60 minutes at 37°C, 5% CO<sub>2</sub>. Then the cells were washed in wash buffer and fixed with 1% paraformaldehyde. The cells were analyzed by flow cytometry with the fluorescein measured on the FL1 channel.

**Measurement of the mitochondrial membrane potential:**

**[0071]** The loss of mitochondrial membrane potential (MMP) as a hallmark of apoptosis was measured using the MITOPROBE JC-1 Assay Kit from Invitrogen (Carlsbad, CA). The cationic

dye JC-1 (5,5', 6,6'-tetrachloro-1,1', 3,3'-tetraethylbenzimidazolylcarbocyanine iodide) exists in healthy cells as a green monomer in the cytosol and also accumulates as red aggregates in the mitochondria. In apoptotic and necrotic cells, JC-1 remains only in the cytoplasm due to mitochondrial depolarization, which can be detected by flow cytometry as a decrease in the red/green fluorescence intensity ratio. CD8+ Jurkat cells or activated T lymphocytes were incubated in PBS containing 2  $\mu$ M of JC-1 for 30 minutes at 37°C, 5% CO<sub>2</sub>. An aliquot of the cells was treated with 50  $\mu$ M of the mitochondrial uncoupler carbonyl cyanide 3-chlorophenylhydrazone (CCCP) during the staining period as a positive control for mitochondrial depolarization. The cells were analyzed using a flow cytometer immediately after staining.

#### **Evaluation of apoptosis-related proteins:**

**[0072]** Expression of anti-apoptotic proteins Bcl-2, Bcl-xL, FLIP and Mcl-1 and the pro-apoptotic proteins Bax, Bim and Bid was investigated in CD8+ Jurkat cells or activated primary T lymphocytes using multicolor flow cytometry. The cells were first stained for surface T-cell markers as described above. For intracellular staining of apoptosis-related proteins the cells were fixed with 1% (v/v) paraformaldehyde in PBS at RT for 10 minutes and then permeabilized with saponin (0.1% v/v in PBS) for 15 minutes at 4°C. Next, the cells were stained for 30 minutes at 4°C with FITC- or PE-conjugated antihuman Bcl-2, Bax and Bcl-xL or unconjugated antibodies for FLIP, Bim, Bid or Mcl-1, followed by a wash with 0.1% saponin. Samples stained with unconjugated antibodies were further incubated with a FITC-conjugated goat anti-rabbit IgG for 15 minutes at room temperature. After washing with 0.1 % saponin, cells were fixed in 1% (v/v) paraformaldehyde. Isotype control matched antibodies were used for both surface and intracellular controls and all antibodies were pre-titered on fresh PBMC.

#### **TUNEL assay:**

**[0073]** DNA fragmentation was measured using the In Situ Cell Death Detection Kit, TMR red (Roche, Indianapolis, IN). Briefly, cytopsin preparations (100,000 cells/ slide) of MV- and IRX-2 treated T cells were air-dried and fixed with 4% (v/v) paraformaldehyde (PFA) in PBS for 1 hour at RT. Slides were rinsed with PBS and incubated with permeabilization solution (01% Triton X-100 in 0.1 % sodium citrate) for 2 minutes on ice. Then the slides were washed twice with PBS and incubated with 20  $\mu$ l of the TUNEL reaction mixture for 1 hour at 37°C in a humidified chamber in the dark. Then the samples were washed extensively with PBS and incubated in a medium with 4', 6-diamidino-2-phenylindole (DAPI; Vector Laboratories, CA) to trace cell nuclei. Slides were evaluated in a Nikon Eclipse E-800 fluorescence microscope under x200 magnification. For digital image analysis, Adobe Photoshop 6.0 was used. A minimum of 300 cells were randomly counted in a microscopic field to determine the percentage of cells with DNA fragmentation.

#### **Statistical analysis:**

**[0074]** Statistical analysis was performed using the Student's t-test. P values <0.05 were considered significant.

#### **EXAMPLE 1**

##### **Example 1**

##### **IRX-2 protects both Jurkat T cells and primary T lymphocytes from cell death mediated by a variety of apoptosis-inducing agents.**

**[0075]** To determine whether IRX-2 protects T cells from apoptosis mediated by tumor-derived microvesicles (MV), CD8+ FasL-sensitive Jurkat cells were pre-incubated with a 1:3 dilution of IRX-2 (approximately 4 ng/mL or 90 IU/mL IL-2) for 24 hours and subsequently treated them with 10 µg of tumor-derived MV (10 µg), CH-11 (400 ng/mL) or staurosporine (1 µg/mL) for 3 hours. As shown in Applicants' previous studies, the co-incubation of Jurkat cells with MV caused marked apoptosis, demonstrated by enhanced Annexin V binding (FIGURES 4A and 4C) and binding of FITC-VAD-FMK indicative of caspase activation (FIGURES 4B and 4D). Dead cells (7-AAD+) were excluded and the gate was set on 7-AAD negative CD8+ Jurkat cells. Upon pre-incubation of Jurkat T cells with IRX-2, the MV-induced apoptosis, as detected by both assays, was significantly reduced (FIGURES 4A-4D).

**[0076]** Interestingly, it was found that IRX-2 was effective not only against MV-induced apoptosis, but also provided protection of Jurkat T cells against FasL-induced (CH-11-Ab) and cytotoxic drug-induced (staurosporine) apoptosis. FIGURES 12C-12D shows IRX-2 significantly reduced apoptosis induced by each of these agents as measured by decreased Annexin V binding (FIGURE 4C) and by reduced caspase activation (Figure 12D). Results shown in FIGURE 4C and FIGURE 4D are representative of 3 independent experiments (\*p<0.05; \*\* p<0.002).

**[0077]** IRX-2-mediated protection was also observed when using primary blood-derived CD8+ and CD4+ T lymphocytes. The data in Table 1 illustrates the protective effect of IRX-2 on both MV- or CH-11-induced apoptosis as indicated by decreases in caspase activation in these cells (Table 1). Similar decreases of Annexin V binding were observed with IRX-2 (data not shown). CD8+ T cells showed a significantly greater sensitivity to MV-induced apoptosis than CD4+ T cells, but in both these subsets, IRX-2 pre-treatment provided a strong protection against MV-induced apoptosis, as determined by a total decrease in the percentage of T cells with caspase-activation. IRX-2 also protected both cell subsets from CH-11 Ab induced apoptosis

(Table 1). Taken together, these findings indicate that IRX-2 effectively protects primary T cells and cell lines from MV- or anti-Fas CH-11 Ab-induced apoptosis as well as from intrinsic apoptosis associated with staurosporine-induced mitochondrial changes. Such results strengthen the argument that IRX-2 provides significant protection from several different types of apoptotic stimuli including that derived from tumors as well intrinsic mechanisms that may be induced by chemotherapy, radiotherapy or viral infection for example.

Table 1. IRX-2 protects activated peripheral blood CD8+ and CD4+ T-lymphocytes from MV- and Fas-induced apoptosis<sup>a</sup>

	CD8+ cells		CD4+ cells	
	mean % of FITC-VAD-FMK+ cells ± SD	p-value <sup>b</sup>	mean % of FITC-VAD-FMK+ cells ± SD	p-value <sup>b</sup>
untreated cells	14.8 ± 4.8		12.6 ± 2.3	
no IRX-2 + CH-11 Ab	52.8 ± 4.9		41.2 ± 9.8	
+ IRX- + CH-11 Ab	15.0 ± 3.5	0.0010	15.4 ± 6.1	0.0510
no IRX-2 + MV	68.9 ± 10.4		49.8 ± 8.0	
+ IRX-2+ MV	26.5 ± 10.3	0.0006	13.9 ± 6.4	0.0211

<sup>a</sup> Activated CD8+ or CD4+ cells were pre-incubated with IRX-2 for 24 hours (at 1:3 final dilution, contains 90 IU/ml IL-2; see Materials and Methods for add'l cytokine conc. details) and then treated with 10 µg MV or CH-11 antibody (Ab) (400 ng/mL) for an additional 24 hours. Cells were analyzed for caspase activation by FITC-VAD-FMK staining via flow cytometry. Results are mean percentage ± SD of 3 independent experiments.

<sup>b</sup> The p values are for differences between no IRX-2 and +IRX-2 treated cells.

## EXAMPLE 2

### IRX-2-mediated protection from apoptosis is time- and concentration -dependent.

**[0078]** To better understand the protective effects of IRX-2 on T cells, CD8+ Jurkat cells were pre-incubated with IRX-2 (fixed dilution of 1:3 = 90 IU/ml IL-2) for incrementally longer time periods (0-24 hours) or with increasing concentrations of IRX-2 (as indicated) for a fixed 24 hour period and subsequently treated with MV (10 µg) for 3 hours (FIGURES 5A and 5B, respectively). Apoptosis was assessed using FITC-VAD-FMK staining of activated caspases by flow cytometry. IRX-2 was found to block MV-induced apoptosis, and this inhibition was time-

dependent, as extending the time of the pre-incubation with IRX-2 intensified its protective effects. A maximal inhibition was observed after 24 hours of MV treatment (FIGURE 5A). Pre-incubation of T cells with different IRX-2 concentrations showed a dose-dependent inhibition of apoptosis caused by MV (FIGURE 5). At the highest possible concentration (i.e., undiluted IRX-2), IRX-2 completely inhibited the induction of apoptosis by MV (FIGURE 5B). Results are mean percentage  $\pm$  SD of 4 independent experiments. The fact that IRX-2-mediated inhibition is both time and concentration dependent demonstrates pharmacologically that the effects are specific to the drug.

**[0079]** It was also desired to determine whether IRX-2 could protect T cells from apoptotic cell death once the apoptotic cascade had been initiated. To address this question, CD8+ Jurkat cells were untreated, treated with IRX-2 (1:3 dilution) for 24 hours (+IRX), MV for 3 hours (+MV), pre-incubated with IRX-2 for 24 hours and then treated with MV (10  $\mu$ g) for 3 hours (+IRX→MV) or first incubated with MV and then treated with IRX-2 (+MV→IRX-2) or incubated with both agents simultaneously (+MV and IRX) for 3 hours or 24 hours, respectively. Activation of caspases was analyzed by flow cytometry. Results are mean percentage  $\pm$  SD from a representative experiment of 3 performed (\* $p<0.002$  compared to MV-treated sample). In comparison to the effects of IRX-2 treatment prior to the addition of MV, apoptosis was reduced by about 50% after simultaneous co-incubation of T cells with MV + IRX-2 (FIGURE 6). When IRX-2 was added 3 hours after treatment with MV, the protective effect of IRX-2 was completely abrogated. Since IRX-2 was obviously not able to overcome the apoptotic cascade already initiated by MV, it acts through a protective mechanism rather than through a reversal of ongoing apoptotic processes initiated by MV.

### EXAMPLE 3

#### **Comparison of the protective effect of IRX-2 with the effect of the survival cytokines IL-7 and IL-15: caspase-activation in Jurkat CD8+ cells after treatment with tumor-MV.**

**[0080]** Jurkat CD8+ cells were plated at a density of 300,000 cells/100  $\mu$ L/well in a 96 well-plate and incubated for 24 hours with IRX-2 (1:3 final concentration), IL-7 (10ng/mL), IL-15 (10 ng/mL), or both cytokines (10 ng/ML each), respectively. The cells were treated for 3 hours with PCI-13/FasL-MV (15  $\mu$ g). Jurkat CD8+ cells heated for 10 minutes at 56 degrees C were used as a positive control. The cells were harvested, washed in 1 mL PBS, resuspended in 500  $\mu$ L PBS, and stained with 5  $\mu$ M VAD-FITC at 37 degrees C for 20 minutes. Then the cells were washed in PBS and stained for 15 minutes for CD8-PE-Cy5. After washing, the cells were fixed in 1% PFA and analyzed by multiparametric flow cytometry.

**[0081]** The percent of activated caspase-VAD-FITC binding CD8+ Jurkat cells were determined for each treatment group as shown in FIGURE 7. The MV-induced apoptosis (no IRX-2 lane; 50% cells undergoing apoptosis) was dramatically inhibited by pre-treatment with

either IRX-2 alone (11% apoptotic cells = 4.5 fold reduction) or a mixture of IL-7 and IL-15 (5% apoptotic cells = 10 fold reduction). Singly, neither IL-7 nor IL-15 alone was able to reduce the level of apoptosis below the control MV-induced level. IRX-2 does not contain either IL-7 or IL-15 both of which are recognized as potent "survival" factors of lymphoid cells. This demonstrates that the apoptosis-inhibiting activity of IRX-2 is the result of a synergistic combination of biologically active components and cannot be reproduced by a single recombinant cytokine.

#### EXAMPLE 4

##### **Protective effect of IRX-2 and survival cytokines IL-7 and IL-15: Caspase-activation in activated CD8+ and CD4+ T-cells after treatment with apoptosis inducers.**

**[0082]** Non-adherent cells from leukocyte units (buffy coats) were thawed, 60x10<sup>6</sup> cells (in 60 mL 10% FCS, RPMI-medium) were activated with CD3/CD28 Dynal beads (1 bead/cell) for 3 days. After activation, cells were washed and CD8+ and CD4+ cells were isolated by magnetic separation (positive selection, Miltenyi MicroBeads). 300,000 cells were plated in 96 well-plates in 100 µL/well and incubated with IRX-2 (1:3) or the cytokines IL-7 and IL-15 (100 ng/mL) for 24 hours. The cells were then treated for an additional 24 hours with PCI-13/FasL-MV (15 µg) (FIGURES 8A, 8B) or CH-11 Ab (400 ng/mL) (FIGURES 9A, 9B) to induce apoptosis.

**[0083]** After incubation, the cells were harvested, washed in 1 mL PBS, resuspended in 300 µL PBS and stained with 3 µM VAD-FITC at 37 degrees C for 20 minutes. The cells were washed in PBS and stained for 15 minutes for CD8-PE-Cy5 or CD4-PE-Cy5, as indicated. After washing, the cells were fixed in 1% PFA and analyzed by multiparametric flow cytometry.

**[0084]** In response to apoptosis induction via tumor cell line PCI-13/FasL-MV, the percentage of cells binding caspase-VAD-FITC (indicator of cells were undergoing apoptosis) was determined for pre-activated human peripheral blood-derived CD4+ (FIGURE 8A) or CD8+ (FIGURE 8B) cells that had been pre-incubated with IRX-2 alone or the indicated recombinant cytokines. These data show that IRX-2 is able to inhibit apoptosis as seen previously on Jurkat CD8+ cells (Figure 4-6) however the degree of inhibition appears less than what was observed on Jurkat cells. In this experimental situation where primary human (non-cell line) T cells are employed, IL-7 and IL-15 were similarly effective compared to IRX-2, either alone or combined. This apparent difference is most likely related to the use of a heterogeneous T cell population from peripheral blood rather than the cloned homogeneous Jurkat cell line. Nevertheless, in either situation and on both CD4+ and CD8+ populations, IRX-2 did indeed inhibit apoptosis in response to the tumor-derived MV.

**[0085]** In an extension to the above findings, a similar experiment was undertaken to evaluate percent caspase-VAD-FITC binding of pre-activated human peripheral blood-derived CD4+

(FIGURE 9A) or CD8+ (FIGURE 9B) cells in this case treated with an alternative apoptosis inducer, anti-Fas antibody (CH-11). In this context, IRX-2 is the most effective at inhibiting apoptosis induction compared to either IL-7 or IL-15 or both combined. This was true for both the CD4+ and CD8+ populations taken from normal blood donors. Such results strengthen the argument that IRX-2 provides significant protection from several different types of apoptotic stimuli including that derived from tumors.

#### EXAMPLE 5

##### **The survival signals promoted by IRX-2 greater than the protective effects of other recombinant survival cytokines**

**[0086]** Since IL-2 is a principal cytokine in IRX-2 (~ 90 IU/mL IL-2 at the 1:3 dilution used), the observed anti-apoptotic activity of IRX-2 could be in part IL-2-dependent. On the other hand, synergy with other cytokines present in IRX-2 could promote survival. Activated CD8+ and CD4+ T-cells were incubated with either 100 IU/mL of recombinant human IL-2, a dose approximating that present in the 1:3 IRX-2 dilution, or IRX-2 (~90 IU/mL at 1:3) and compared for the ability to inhibit MV- or CH-11 antibody-induced apoptosis. As shown in Table 2A, IL-2 had a similar protective effect against MV-induced apoptosis as IRX-2 in CD8+ T cells, but had a lower protective effect in CD4+ T cells. In terms of protection against CH-11Ab-induced apoptosis, IL-2 was significantly much less effective than IRX-2 in enhancing survival of CD4+ T cells and had almost no effect in CD8+ T cells (Table 2B). These findings indicate that the survival-enhancing potential of IRX-2 is greater than that of its main cytokine IL-2 and that support by other cytokines that are present in IRX-2 at very low physiological concentrations contribute to these effects.

**[0087]** It is likely that cytoprotective effects of IL-2 in IRX-2 are enhanced by the presence of IFN $\gamma$  and GM-CSF, which in combination, could mediate immuno-potentiating effects. The role of other components of IRX-2 (e.g., IL-1 $\alpha$ , IL-6, IL-8, TNF $\alpha$ ) in promoting T-cell survival is less clear, although studies have shown that, depending on tissue location and concentration, some of these pro-inflammatory cytokines can also support anti-tumor immune responses. It is important to note that a functional synergism amongst the various components of IRX-2 was previously described, demonstrating, for example, that IRX-2 was able to induce maturation of dendritic cells to a greater extent than comparable levels of TNF $\alpha$  alone.

**[0088]** Additionally, the protective effect of IRX-2 was compared with the activity of recombinant IL-7 and IL-15, both potent survival cytokines for lymphocytes, which are not present in the IRX-2 mixture. Pre-incubation of T cells with these cytokines at a concentration of 10 ng/mL, alone or in combination, provided protection from MV-induced or CH-11 Ab-induced apoptosis in all cases, although to different extents (Table 2A and B). IL-7 alone only weakly inhibited both CH-11 Ab- and MV-induced apoptosis in both cells subsets in comparison

to IRX-2. IL-15 alone was as potent as IRX-2 in protection against MV-induced apoptosis but provided a weaker survival signal against CH-11 Ab-induced apoptosis. A combination of both cytokines blocked apoptosis in CD8+ and CD4+ cell subsets, and the level of apoptosis inhibition was similar to that mediated by IRX-2, but only in case of MV-induced apoptosis (Table 2A and B). Thus, the protective effects of IRX-2 were comparable to or in some cases (e.g., protection of CD8+ cells) even stronger than those of the recombinant survival cytokines, IL-7 and IL-15 in protecting CD4+ cells. IRX-2 was found to be significantly more effective than recombinant IL-7 in protecting activated CD4+ and CD8+ T cells from MV- and CH-11 Ab-induced apoptosis and had similar protective effects as IL-15. Among the cytokines tested, IRX-2 had the greatest survival potency when CH-11 Ab was used to induce apoptosis, implying protection against receptor-mediated apoptosis. It should be noted that the concentrations of IL-7 and IL-15 used in these experiments are relatively high and not physiological levels, again suggesting a strong synergy between the components of IRX-2.

**Table 2. Anti-apoptotic effects of IRX-2 in comparison to IL-2, IL-7 and IL-15 in (a) MV-induced or (b) CH-11 Ab-induced<sup>a</sup> apoptotic primary T cells.**

<b>A. MV-induced apoptosis</b>				
	CD8+ cells		CD4+ cells	
	mean % of FITC-VAD-FMK+ cells ± SD	p-value <sup>b</sup>	mean % of FITC-VAD-FMK+ cells ± SD	p-value <sup>b</sup>
control	21.8 ± 3.9		14.3 ± 5.0	
no IRX-2 + MV	63.2 ± 4.5		52.8 ± 8.7	
+ IRX-2 + MV	20.6 ± 0.8	0.0006	10.2 ± 0.4	0.0038
+ IL-7 + MV	49.5 ± 3.5	0.0004	34.5 ± 1.9	0.0124
+ IL-15 + MV	16.8 ± 6.2	0.0044	16.7 ± 2.1	0.0072
+ IL-7/IL-15 + MV	11.8 ± 6.2	0.0036	11.9 ± 0.8	0.0031
+ IL-2 + MV	21.9 ± 2.7	0.0002	22.2 ± 2.7	0.0113

<b>B. CH-11 Ab-induced apoptosis</b>				
	CD8+ cells		CD4+ cells	
	mean % of FITC-VAD-FMK+ cells ± SD	p-value <sup>b</sup>	mean % of FITC-VAD-FMK+ cells ± SD	p-value <sup>b</sup>
control	12.3 ± 2.8		11.4 ± 1.3	
no IRX-2 + MV	50.0 ± 0.2		46.8 ± 3.0	
+ IRX-2 + MV	13.4 ± 3.0	0.0007	12.0 ± 1.7	0.0001

**B. CH-11 Ab-induced apoptosis**

	CD8+ cells		CD4+ cells	
	mean % of FITC-VAD-FMK+ cells ± SD	p-value <sup>b</sup>	mean % of FITC-VAD-FMK+ cells ± SD	p-value <sup>b</sup>
+IL-7 + MV	37.7 ± 1.4	0.0015	31.8 ± 10.6	
+ IL-15 + MV	28.8 ± 3.1	0.0020	21.1 ± 5.3	0.0086
+ IL-7/IL-15 + MV	24.2 ± 4.9	0.0028	20.2 ± 0.1	0.0010
+ IL-2 + MV	44.2 ± 6.9		31.7 ± 3.0	0.0128

<sup>a</sup> Activated primary CD8+ and CD4+ T-cells were pre-incubated with IRX-2 (1:3 dilution, includes ~90 IU/ml IL-2, see Materials & Methods.), recombinant human IL-2 (100 IU/mL), IL-7 (10 ng/mL), IL-15 (10 ng/mL) or IL-7 and IL-15 (both 10 ng/mL) for 24 hours and then treated with 10 µg MV or 400 ng/mL CH-11 antibody (Ab) for an additional 24 hours. Activation of caspases was analyzed by flow cytometry. Data are mean percentages of FITC-VAD-FMK+ cells ± SD.

<sup>b</sup> The p values refer to significant differences between cells pre-treated with IRX-2 compared to MV alone or cells pre-treated with the cytokine indicated compared to those pre-treatment with IRX-2.

**EXAMPLE 6**

**IRX-2 provides protection against MV-induced apoptosis at various steps in the apoptotic pathway.**

**[0089]** Having shown IRX-2-mediated protection extends to primary T cells as well as the Jurkat cell line and several inducing agents, we continued by evaluating the ability of IRX-2 to inhibit downstream steps in the apoptotic process using the co-incubation of Jurkat cells with MV. CD8+ Jurkat cells were either untreated, incubated with 10 µg MV for 3 hours or pre-treated for 24 hours with IRX-2 (1:3 dilution) and then incubated with MV for 3 hours. CD8+ Jurkat cells were also co-incubated with MV and 20 µM of the pan-caspase inhibitor Z-VAD-FMK (zVAD) or co-incubated with MV and the anti-Fas neutralizing mAb ZB4 (10 µg/mL) (controls). Results are the mean MFI ± SD of 3 independent experiments. As shown in FIGURE 13A, MV-treatment of Jurkat cells led to a very strong increase in the mean fluorescent intensity (MFI) of caspase-3/-7-FAM, a dye which specifically binds to activated caspase-3 and caspase-7, the main effector caspases of both receptor- and mitochondrial-mediated apoptosis. Pre-treatment with IRX-2 completely prevented the MV-induced induction of caspase-3 and -7 activity as well as the irreversible caspase inhibitor zVAD and the anti-Fas neutralizing monoclonal antibody (mAb) ZB4. Caspase-3 activation by MV was also detected

by Western immunoblot analysis, where a dramatic decrease in the protein level of the inactive caspase-3 pro-form and a simultaneous increase of the active cleaved form was observed in MV-treated Jurkat T cells over 24 hours (FIGURE 10B, lanes 3 and 4). IRX-2 pre-treatment effectively blocked induction of the active cleaved form (FIGURE 10B, lanes 5 and 6). The cells were either untreated, treated with IRX-2 (1:3 dilution) for 24 hours (+IRX), treated with MV (10 µg) for 3 hours (+MV 3 hours) or 24 hours (+MV 24 hours) or pre-incubated with IRX-2 for 24 hours and then treated with MV (10 µg) for 3 hours or 24 hours (+IRX→MV). Whole cell lysates of the cells were separated on SDS-PAGE and transferred to PVDF membranes for subsequent Western blotting. Activation of caspase-3 is shown as a decrease in the inactive pro-form and the appearance of the active subunits p17 and p10. Results are representative of 3 Western blots.

**[0090]** In addition, IRX-2 blocked the MV-induced loss of mitochondrial membrane potential (MMP) in Jurkat T cells (FIGURES 11A and 11B). This block was comparable to that provided by the two inhibitors z-VAD and ZB4 (FIGURE 11B). CD8+ Jurkat cells were analyzed by flow cytometry for a decrease in red fluorescence of the cationic dye JC-1, indicating a loss of MMP. Percentage of JC-1 red-negative cells were determined in cultures of CD8+ Jurkat cells after no treatment, 24 hours treatment with MV (10 µg) alone (no IRX) or pre-treated for 24 hours with IRX-2 (1:3 dilution) or MV in combination with the apoptosis-inhibitor Z-VAD-FMK (pan-caspase inhibitor; conc) or ZB4 (anti-Fas neutralizing mAb, conc/dose). Cells treated with 50 µM carbonyl cyanide 3-chlorophenylhydrazone (CCCP), a protonophore that dissipates the H<sup>+</sup> gradient across the inner mitochondrial membrane, were used as a positive control. Results are mean ± SD of 3 independent experiments (\*p<0.005; \*\*p<0.002 compared to sample without IRX-2).

**[0091]** Finally, IRX-2 pre-treatment significantly reduced the MV-induced nuclear DNA fragmentation as detected by TUNEL assay (FIGURES 12A and 12B), representing the final step in the apoptotic process (p<0.0002; FIGURE 12B). CD8+ Jurkat cells were either untreated (a), incubated for 24 hours with IRX-2 alone (b) or MV alone for 24 hours (c) or pre-incubated with IRX-2 for 24 hours and subsequently treated with MV for 24 hours (d) and then stained by the TUNEL method to reveal DNA strand breaks (red nuclei) indicative of apoptosis. A minimum of 300 CD8+ Jurkat cells were counted for each treatment group. Results are expressed as the mean percentage ± SD of two independent experiments (\*p<0.0002 compared to MV-treated sample). This data therefore confirms that IRX-2 exhibits protective effects at each of the relevant steps that culminate in T cell death.

#### EXAMPLE 7

**IRX-2 protects T cells from MV-induced down-regulation of JAK3 and STAT5 expression.**

**[0092]** It has been previously observed that MV derived from sera of patients with cancer down-regulate expression of molecules mediating the common  $\gamma$  chain cytokine receptor signaling pathway, including JAK3 and STAT5. Since this pathway is essential for the development, maintenance and survival of lymphocytes, and in particular, of CD8+ cells, effects of MV and IRX-2 on JAK3 and STAT5 expression in CD8+ Jurkat cells were next examined.

**[0093]** CD8+ Jurkat cells were untreated or treated with IRX-2 (1:3 dilution) and MV in different combinations. Whole cell lysates of cells from each treatment group were separated on SDS-PAGE and transferred to PVDF membranes for subsequent Western blotting. The expression levels of JAK3, phosphorylated and total STAT5, CD3 $\zeta$  and FLIP were analyzed by probing membrane with specific antibodies. Reprobing with  $\beta$ -actin antibody confirmed equal protein loading.

**[0094]** The results shown are representative of 4 experiments performed. As previously observed, MV caused a significant down-regulation of JAK3 in T cells (FIGURE 18, panel 1, compare lanes 1 and 3), which intensified with the extended time of co-incubation (FIGURE 18, panel 1, lanes 3 and 4). While IRX-2 alone did not increase JAK3 expression (FIGURE 18, panel 1, compare lanes 1 and 2), it was able to completely reverse the MV-induced JAK3 down-regulation and restore its expression (FIGURE 18, panel 1, compare lanes 3, 4 with lanes 5, 6). Furthermore, IRX-2 caused a strong activation of STAT5, a JAK3 signal transducer, as indicated by phosphorylation of this protein (FIGURE 18, panel 2, lane 5). This dramatic activation of STAT5 was sustained even after prolonged (24 hours) incubation with MV (FIGURE 18, panel 2, lane 6). Additionally, a loss in CD3- $\zeta$  expression in T cells was observed after MV treatment. Here again, pre-incubation with IRX-2 protected T lymphocytes from MV-mediated CD3- $\zeta$  down-regulation (FIGURE 18, panel 4, compare lanes 3, 4 with lanes 5,6).

**[0095]** These changes are all consistent with IRX-2 mediating protection from apoptosis via the cytokines present in IRX-2, especially via the primary cytokine IL-2 which is known to signal through the IL-2 receptor and the downstream intracellular signaling molecules Jak3/Stat5. These data elucidate downstream molecular targets of IRX-2 that are central in sending survival and stimulation signals in lymphoid cells.

#### **EXAMPLE 8**

##### **IRX-2 reverses the MV-induced imbalance of pro- and anti-apoptotic proteins.**

**[0096]** To further examine the mechanisms through which IRX-2 promoted protection of T cells from apoptosis, expression levels of various pro- and anti-apoptotic proteins were measured in activated, MV-treated T lymphocytes and CD8+ Jurkat cells in the presence or absence of IRX-2 by quantitative flow cytometry. Table 3 shows expression levels of several

apoptosis-related proteins as mean fluorescence intensity (MFI) in activated CD8+ cells before and after MV treatment. Incubation of T cells with MV caused a significant up-regulation of the pro-apoptotic proteins Bax and Bim, and a concurrent down-regulation of anti-apoptotic Bcl-2, Bcl-xL, FLIP and Mcl-1 (Table 3A). This is consistent with Applicants' previous findings indicating that MV induce apoptosis of T cells. While absolute protein levels are important, it is the ratio of pro-/anti-apoptotic protein levels present in the cell that actually determines cell fate. Thus, changes in these ratios are much more informative of cell state (Table 3B). Dramatic changes of the Bax/Bcl-2, Bax/Bcl-xL and Bim/Mcl-1 ratios upon treatments with MV or IRX-2+ MV were observed. A significant pro-apoptotic shift in these ratios occurred in CD8+ cells upon incubation with MV. In contrast, pre-treatment of T cells with IRX-2 caused a dramatic decrease in these ratios rendering them congruent with those present in untreated cells. (Table 3B), as shown in FIGURE 14A. Activated peripheral blood (PB) CD8+ cells were pre-incubated with IRX-2 (at 1:3 dilution) for 24h and then treated with 10 µg MV for additional 24h. Expression levels (mean fluorescence intensity) of different pro- and anti-apoptotic protein were measured by quantitative flow cytometry. As shown in FIGURE 14B IRX-2 treatment is able to maintain levels of the anti-apoptotic proteins Bcl-2 and Mcl-1 after MV treatment and down regulates expression of the pro-apoptotic protein Bax. MV and IRX-2 had little or no effect on the expression of pro-apoptotic FasL and Bid (data not shown). Similar results were obtained after IRX-2 incubation and MV treatment of activated primary CD4+ cells and CD8+ Jurkat cells.

**[0097]** The balance of pro- versus anti-apoptotic proteins determines whether the cell will complete the apoptotic process resulting in death of the cell. IRX-2 reverses the MV-induced shift toward apoptosis leading to protection from apoptosis. The fact that IRX-2 works to up-regulate core anti-apoptotic proteins such as BCL-2, demonstrates that it is a general inhibitor of apoptosis in lymphoid cells and is beneficial in protecting these cells from a wide variety of tumor derived factors.

**Table 3.** MV and IRX-2 modulate the expression of pro- and anti-apoptotic proteins.

The mean fluorescence intensity  $\pm$  SD (a) and ratios (b) of pro- and anti-apoptotic proteins of MV- and IRX-2-treated activated CD8+ cells<sup>a</sup> are indicated below.

**A.**

	untreated		+ MV		+ IRX-2 + MV	
	mean fluorescence intensity $\pm$ SD	mean fluorescence intensity $\pm$ SD	p value (compared to untreated sample)	mean fluorescence intensity $\pm$ SD	p value (compared to MV-treated sample)	
Bcl-2	7.7 $\pm$ 0.4	1.9 $\pm$ 0.1	0.0008	4.8 $\pm$ 0.6	0.0049	
Bax	17.9 $\pm$ 1.2	40.0 $\pm$ 1.5	0.0001	26.8 $\pm$ 2.3	0.0003	
Bcl-xL	20.1 $\pm$ 0.1	8.2 $\pm$ 0.4	0.0001	11.0 $\pm$ 0.8	0.0019	
FLIP	42.4 $\pm$ 0.6	17.5 $\pm$ 0.6	0.0002	25.5 $\pm$ 2.0	0.0030	
Bim	8.1 $\pm$ 0.3	16.7 $\pm$ 1.6	0.0016	9.2 $\pm$ 0.3	0.0020	
Mcl-1	37.5 $\pm$ 3.8	7.1 $\pm$ 1.1	0.0004	35.1 $\pm$ 1.6	0.0003	

■

b.

	<u>Bax/Bcl-2 ratio</u>		<u>Bax/Bcl-xL ratio</u>		<u>Bim/Mcl-1 ratio</u>	
	mean $\pm$ SD	p value <sup>b</sup>	mean $\pm$ SD	p value <sup>b</sup>	mean $\pm$ SD	p value <sup>b</sup>
untreated	2.3 $\pm$ 0.6		0.89 $\pm$ 0.3		0.22 $\pm$ 0.3	
+MV	18.6 $\pm$ 1.2	0.0004	4.32 $\pm$ 0.5	0.0001	2.35 $\pm$ 0.2	0.0011
+ IRX-2 + MV	5.58 $\pm$ 0.9	0.0002	2.44 $\pm$ 0.4	0.0003	0.26 $\pm$ 0.1	0.0009

<sup>a</sup> Activated peripheral blood (PB) CD8+ cells were pre-incubated with IRX-2 (at 1:3 dilution; containing ~ 4 ng/ml or 90 IU/ml IL-2) for 24 hours and then treated with 10  $\mu$ g MV for additional 24 hours. Expression levels (mean fluorescence intensity) of different pro- and anti-apoptotic protein were measured by quantitative flow cytometry. The data are means  $\pm$  SD obtained in 3 different experiments.

<sup>b</sup> The p values indicate significant changes in ratios between untreated and MV-treated or IRX-2 + MV-treated cells.

## EXAMPLE 9

### The Akt/PI3K-pathway is the main downstream target of anti-apoptotic activity of IRX-2.

**[0098]** The Akt/PI3K signaling pathway is recognized as one of the most critical pathways in regulating cell survival. Since our findings showed a substantial influence of IRX-2 on several key proteins of the Bcl-2-family, which could be regulated by Akt/PKB, we measured the activation of Akt-1/2 in response to MV and/or IRX-2 using an antibody specific for one of the two major regulatory phosphorylation sites, phosphoserine 473. CD8+ Jurkat cells were untreated or treated with IRX-2 and MV (10  $\mu$ g) in different combinations as indicated. Whole cell lysates of cells from each treatment group were separated on SDS-PAGE and transferred to PVDF membranes for subsequent Western blotting. The activation of Akt-1/2 was analyzed by immunoblotting with Ser473-specific anti-phospho Akt mAb. Reprobing with a total-Akt antibody confirmed equal protein loading. Results shown are representative from one experiment out of 3 performed.

**[0099]** In untreated CD8+ Jurkat cells (control) Akt-1/2 was constitutively phosphorylated to a level characteristic of Jurkat cells (FIGURE 20A, panel 1, lane 1). Pre-incubation with IRX-2 did not enhance basal Akt-phosphorylation (FIGURE 15A, panel 1, lane 2). However, when the cells were treated with MV, a dramatic, time-dependent dephosphorylation of Akt-1/2 was observed (FIGURE 20A, panel 1, lanes 3 and 4). A time-course study with 10  $\mu$ g of MV showed that Akt dephosphorylation started at 3 hours of incubation and intensified over time (data not shown). Pre-treatment of Jurkat cells with IRX-2 completely inhibited MV-induced dephosphorylation of Akt-1/2 at both 3 and 24 hours of treatment (FIGURE 215A, panel 1,

lanes 5 and 6).

**[0100]** This pronounced pro-survival effect of IRX-2 on CD8+ Jurkat cells, which clearly counteracted the MV-induced Akt inactivation, indicated that Akt might serve as the main downstream target of IRX-2 signaling. To confirm this hypothesis, CD8+ Jurkat cells were pre-incubated prior to IRX-2 and MV treatment with a small molecule inhibitor specific for Akt, Akti-1/2, and measured the levels of T-cell apoptosis. CD8+ Jurkat cells were pre-incubated with IRX-2 for 24h or left untreated. Then cells were treated with an Akt inhibitor, Akti-1/2 at different concentrations (0-5  $\mu$ M) for 1 hour prior to the addition of MV for additional 3 hours. The level of apoptosis was measured by FITC-VAD-FMK staining and flow cytometry analysis. Results are mean percentage  $\pm$  SD obtained in 3 individual experiments (\*p<0.05; \*\*p<0.01 compared to MV-treated sample without IRX-2 and Akt inhibitor).

**[0101]** As shown in FIGURE 15B, pre-treatment of the cells with the Akt inhibitor resulted in a gradual abrogation of the anti-apoptotic effect of IRX-2. At a relatively low inhibitor-concentration of 1  $\mu$ M, the protection from apoptosis provided by IRX-2 was only slightly inhibited. However, it was completely blocked at the inhibitor concentration of 5  $\mu$ M. At these inhibitor concentrations, cell viability was not affected (data not shown). This finding shows that Akt is the main downstream coordinator of the survival signal provided by IRX-2.

## CONCLUSIONS OF EXAMPLES 1-9

**[0102]** Confirming previous findings of the Applicants, it was initially showed that incubation of CD8+ Jurkat cells or activated T lymphocytes with MV induced a significant level of apoptosis. Tumor-derived MV expressing a membrane form of FasL were purified from supernatants of the PCI-13 tumor cell line and co-incubated with CD8+ Jurkat cells or activated peripheral blood (PB) T cells. FasL, the Fas ligand, is a type II transmembrane protein belonging to the tumor necrosis factor (TNF) family. FasL-receptor interactions play an important role in the regulation of the immune system and the progression of cancer. Apoptosis is induced upon binding and trimerization of FasL with its receptor (FasR), which spans the membrane of a cell targeted for death. FasL+ MV induced not only the extrinsic receptor-mediated apoptotic pathway, but also the intrinsic mitochondrial pathway in activated T cells, with accompanying up-regulation of the pro-apoptotic Bcl-2 family members, Bax and Bim. Pre-incubation of CD8+ Jurkat or activated primary T cells with IRX-2 suppressed both apoptotic pathways in a dose- and time-dependent manner. Further, the pre-treatment of T cells with IRX-2 provided protection not only against MV-induced cell death, but also against CH-11 Ab- and staurosporine-induced apoptosis. Since the former induces apoptosis mainly through the death receptor pathway and the latter activates only the mitochondrial pathway, these findings further show that IRX-2 can protect T-cells from activation of both the extrinsic and the intrinsic death pathways.

## EXAMPLE 10 (not according to the invention)

**[0103]** The selection of the dose and schedule for the IRX-2 regimen to be used in experiments was based on studies conducted by IRX Therapeutics. The IRX Therapeutics study was performed in mice immunized with prostate specific membrane antigen (PSMA) peptide conjugate and assessed as increase in footpad swelling. FIGURE 21 shows these data and the characteristic "bell-shaped" curve.

**[0104]** The study was performed in four groups of patients, as shown in Table 4 below. The graph of tumor lymphocyte infiltration and survival for these groups are presented in FIGURES 17 and 18, respectively.

TABLE 4

Regimen	N	Dose of IRX-2 injection (Units)	Injections/day	# days	Cumulative Dose of IRX-2 (Units)
1	4	~38 U	1	10	380 U
2	15	~115 U	1	10	1,150 U
3	10	~115 U	2	20	4,600 U
4	6	~660 U	2	20	26,400 U

**[0105]** In this study, maximum lymphoid infiltration was achieved for patients treated with the 10 days of 115 U IL-2 equivalence/day. Survival was poor in the four patients who received the lowest dose (regimen 1). Similarly, poorer survival was noted in six patients treated with the highest dose. While survival appeared to be comparable for regimens 2 and 3, regimen 2 patients experienced the most significant histological response as measured by lymphoid infiltration.

**[0106]** The dose of IRX-2 to be studied further was subsequently selected as intermediate between the two most active doses investigated (regimens 2 and 3), a dose clearly adequate to achieve significant histological changes in tumor and lymph nodes. Based upon the additional inconvenience of 20 versus 10 days of treatment and the lesser lymphoid infiltration in the patients who received the higher IRX-2 dose, a 10-day injection protocol with bilateral injection (approximately 2300 U total of IRX-2) was selected for the further studies discussed below.

#### **EXAMPLE 11 (not according to the invention)**

**[0107]** A study of the IRX-2 protocol was performed in H&NSCC patients prior to surgery and/or radiotherapy and/or chemoradiotherapy as described in FIGURE 1. IRX-2 was administered bilaterally at 115 Units/site. Twenty seven patients were treated; their demographics summarized in Table 5.

TABLE 5

Number of treated patients	32
Median age (range)	66 (34-86)
M:F ratio	25:7
KPS range	70-100
Patient Characteristics	
- Oral	15
- Larynx	13
- Other	4
Stage at Diagnosis	
- I	1
- II	5
- III	10
- IV	15
NA	1
Stage of primary tumor	No. (%)
T1	1 (4)
T2	15 (56)
T3	6 (22)
T4	5 (19)
TX	0
Nodal stage	No. (%)
N0	5 (19)
N1	8 (30)
N2	14 (52)
N3	0
NX	0

**[0108]** Radiological studies (CT or MRI) were performed at the onset and prior to surgery and reviewed centrally (Perceptive, Waltham, MA). Blood was analyzed centrally (Immunosite, Pittsburgh, PA) at onset and prior to surgery for various leukocyte populations (Table 6 and 7). Surgical samples were sent to a central reference laboratory (Phenopath, Seattle, WA) for evaluation of the histological changes and performance of immunohistochemistry for various leukocyte markers (Table 8). Appropriate laboratory and clinical measurements were

performed to assess toxicology and symptomatic improvement throughout disease-free and overall survival continue to be monitored.

**Clinical results:**

**[0109]** Three patients had objective tumor responses (2PR; 1MR). Four patients showed radiological responses (>12.5% reduction); five patients (N2, N2, N1, N1, N1) were down-staged as nodes detected as tumor-positive at the sites and centrally were shown to be negative in the surgical specimens. Four tumors softened (a positive sign), 14 patients had symptomatic improvement/reduced pain and tenderness, improved swallowing, and less bleeding. Treatment related side effects were generally mild (grade I or II) and infrequent including nausea, vomiting, dry mouth, constipation, injection site pain, headache, myalgia, anemia, and contusion. A single example of dyspepsia grade III was observed. Disease-free and overall-survival are being followed. Most patients have cleared one year and survival curves closely parallel those previously observed by Applicants in studies at the National Cancer Institute of Mexico and appear better than case-matched U.S. and Mexican controls.

**EXAMPLE 12 (not according to the invention)**

**[0110]** Heparinized blood was collected for immunophenotyping studies to determine numbers of immune cell subsets including B, T, NK, and T naïve, T memory, and T effector cells. Fluorescently tagged monoclonal antibodies to the indicated cell surface markers (or corresponding isotope control) were used to stain fresh, unfractionated whole blood.

**[0111]** The stained and fixed samples were then acquired and analyzed by multiparameter flow cytometry using a Beckman Coulter FC500 flow cytometer and CXP TM analysis software. Enumeration of absolute T lymphocyte subsets using this single platform (flow cytometry only) method that employs Flow Count TM beads has been demonstrated to be more accurate than dual (hematology instruments and flow cytometry) platform techniques (Reimann et al., 2000). Table 6 below presents a list of the immune markers analyzed by ImmunoSite and their role in an immunization.

**TABLE 6 - Immune Markers Analyzed & Role in Immune Response**

Cell	Marker	Role
T cell	CD3	Mediates cellular immunity
B cell	CD3- CD19+ CD14-	Mediates humoral immunity
Helper T cell	CD3+ CD4	Makes cytokines, provides B cells "help"
Cytotoxic T cell	CD3+ CD8	Kills tumor cells
Naïve T cell (T <sub>N</sub> )	CD3+ CD45RA+	Antigen naïve or very early post-primary stimulation; lymph node homing ability

Cell	Marker	Role
	CCR7+	
Central Memory T cell (T <sub>CM</sub> )	CD3+ CD45RA- CCR7+	Long-lived memory cell, low effector function; homes to lymph nodes
Effector Memory T cell (T <sub>EM</sub> )	CD3+ CD45RA- CCR7-	Intermediate effector function; shorter half-life <i>in vivo</i> ; seeds tissues/tumors over lymph nodes
Effector T cell (T <sub>EMRA</sub> )	CD3+ CD45RA+ CCR7-	Highest effector function (e.g. cytolysis); localizes best to tissues/tumor

**[0112]** For the purposes of the present invention, only the cell populations directly relevant to evaluating the hypothesis of whether an immunization occurred or not are discussed herein.

**[0113]** The developmental pathways for T lymphocytes, especially CD8+ T cells, have been intensively studied over the last decade with a particular focus on CD8+ T cells since they are most closely associated with effective anti-tumor immunity. Both CD4+ helper T cells and CD8+ cytotoxic T cells can be subdivided into reciprocal CD45RA+ and CD45RO+ subpopulations. CD45RA+ cells have previously been termed naïve T cells; however, more recent work indicates that these T cells in blood comprise naïve T cells as well as more fully differentiated effectors often termed T<sub>EMRA</sub> (Lanzavecchia, 2005; Kaech, 2002). CD45RO+ (CD45RA-) memory T cells can also be subdivided into T central memory (T<sub>CM</sub>) and T effector memory (T<sub>EM</sub>). These sub-classifications are based upon surface expression of additional markers including CCR7 (Sallusto, 1999; Tomiyama, 2004). The developmental pathways of these various T cell subsets and their lineage relationships remain complex. The data and tests for significance are presented in Table 7 below.

**TABLE 7 - Summary of Immunology Assessments & Tests of Significance**

Cell population	N	Mean cells/mL <sup>3</sup>	Std Dev	Baseline to Day 21 Difference	Std Dev	Degrees of Freedom	T value	P value
<b>Baseline</b>								
Lymphocyte Gate	25	1177.5	442.4	-69.6	260.7	24	-1.33	0.1946
B cell	18	275.4	132.2	-74.3	74.8	17	-4.22	0.0006
Helper T cell	25	817.0	330.7	-65.4	184.0	24	-1.78	0.0884
Cytotoxic T cell	25	351.9	193.3	-4.4	87.9	24	-0.25	0.8061
Naïve T cell	25	55.6	89.8	-38.2	76.9	24	-2.49	0.0203

Cell population	N	Mean cells/mL <sup>3</sup>	Std Dev	Baseline to Day 21 Difference	Std Dev	Degrees of Freedom	T value	P value
<b>Baseline</b>								
Central Memory T cell	25	56.9	84.5	-22.8	48.6	24	-2.34	0.0280
Effector Memory T cell	25	689.0	354.7	41.2	223.4	24	0.92	0.3651
Effector Memory RA T cell	25	395.0	250.2	-35.2	132.7	24	-1.33	0.1968

**[0114]** Consistent with the hypothesis that IRX-2 acts on both T cells and DC's to foster activation, maturation, and enhance endogenous tumor antigen presentation to naïve T cells, it was observed that the naïve T cell population (CD3+ CD45RA+ CCR7+) decreased between baseline and Day 21. Naïve T cells are initially activated by recognition of antigen when presented on the appropriate major histocompatibility complex (MHC) molecules by mature DC's. The subsequent steps of generating T cell memory and full effector function are not perfectly defined, but it is clear that different subpopulations of T cells as defined by several markers, i.e. CD45RA/RO and CCR7 have distinct functional properties. For example, CCR7 expression confers the ability of the T cell to home to lymph nodes where the most effective anti-tumor priming occurs.

**[0115]** A significant decline was observed in the naïve T cell population (CD3+ CD45RA+ CCR7+) with population levels of 55.6 cells/mL<sup>3</sup> at baseline falling to 17.4 cells/mL<sup>3</sup> at Day 21 ( $p = 0.02$ ). A loss of naïve T cells results from those cells finding and being stimulated by their respective cognate antigen and the differentiating into an alternative functional population, either of the two memory or full effector populations.

**[0116]** In addition, the central memory T cell population (CD3+ CD45RA- CCR7+) with the CCR7+ conferred lymph node homing propensity, fell from 56.9 cells/ mL<sup>3</sup> at baseline to 34.1 cells/ mL<sup>3</sup> at Day 21 ( $p = 0.028$ ). This too is an indicator that immunization to tumor antigens is taking place in response to IRX-2 therapy. Studies show that the T<sub>CM</sub> population of T cells represents the earlier, more "stem-like" memory population that upon re-stimulation, preferentially homes to the lymph node where it can gain more effector, e.g. cytolytic function. The significant decline seen in this population is consistent with these T<sub>CM</sub> cells exiting the bloodstream and migrating to the draining lymph nodes where they will be further activated.

**[0117]** After an immunization, one would expect other immune cells to be enlisted in the attack on the antigen-bearing offender. Further support to the immunization hypothesis was observed

in that a significant drop ( $p < 0.01$ ) in B cells was observed. B cells are recruited into lymph nodes where they are exposed to antigen and then exit to be found in the tumor where they presumably produce antibodies capable of attacking the tumor directly or supporting antibody-dependent cellular cytotoxicity (ADCC).

**[0118]** The statistically significant changes and trends observed herein strongly show that an immunization of naïve T cells is occurring due to IRX-2 administration. As no other primary interventions were observed in these patients, it is unlikely that these changes occurred at random.

**[0119]** The hypothesis that IRX-2 treatment induces immunization to autologous tumor antigens is also supported by Applicants' published information on H&NSCC lymph node response following IRX-2 treatment as compared to non-randomized normal and H&NSCC control patients (Meneses, 2003). The salient lymph node response features associated with IRX-2 treatment were nodal replenishment and lymphocyte expansion, particularly T lymphocytes, which were shown to be depleted in the lymph nodes of untreated H&NSCC patients (Verastegui, 2002). Nodal expansion that occurs during an immunization presumably due to IRX-2 was also observed to be associated with a reversal of sinus histiocytosis, an apparent dendritic cell functional defect. These changes are consistent with an immunization. A prior study confirms that immunization to tumor antigen occurs at the level of the regional lymph node, not the tumor itself (Maass, 1995).

### **Histology**

**[0120]** When an immunization occurs in lymph nodes, the new killer memory T cells are thought to develop and then exit the nodes through blood vessels, and flow into tissues to patrol for the antigenic target (i.e. the immune target). If the antigenic target is identified, the killer memory T cell will infiltrate the tissue to kill the target. When a cellular immune response is initiated, other immune cells are recruited to participate in the kill and clean-up process.

**[0121]** T lymphocyte infiltration into tumors, particularly of CD45RO+ CD8+ T cells, is evidence of an immunization to tumor antigens and that such infiltration correlates with improved survival in a variety of cancers including H&NSCC, melanoma, colorectal, and ovarian (Wolf, 1986; Pages, 2005; Galon, 2006).

**[0122]** It was hypothesized herein that an IRX-2 induced immunization in lymph nodes would result in lymphocytic infiltrate in the tumor and tumor disruption and the presence of specific immune cells in the tumor would provide evidence of an anti-tumor immune response. It was also hypothesized that an immune response to the tumor would be evidenced by diffuse lymphocytic infiltrate, spanning the tumor's peripheral area to its intratumoral area.

**[0123]** Formalin fixed paraffin embedded blocks or unstained slides from primary tumor biopsy and resection specimens were submitted by the clinical sites to PhenoPath Laboratories

(Seattle, WA) for hematoxylin and eosin ("H&E") and immunohistochemistry staining ("IHC"). Paired samples from 26 IRX-2 study subjects were submitted, 25 were evaluable, and one surgical specimen had no histological evidence of tumor. Two ad-hoc comparator groups of surgical specimens were collected at the end of the study for H&E comparison: 25 surgical specimens from MD Anderson, and 10 surgical specimens from Stony Brook Health Sciences Center, randomly selected from untreated H&NSCC surgical specimens.

**[0124]** Immunohistochemistry staining was performed only on the IRX-2 treated samples to determine the presence of immune markers in the tumor. Their markers are listed in Table 8.

**TABLE 8 - Immune Markers Analyzed by IHC**

Cell	Marker	Role in Immune Response
T cell	CD3	Mediate cellular immunity
B cell	CD20	Produce antibody
Helper T cell	CD4	Make cytokines; help B cells
Cytotoxic T cell	CD8	Kill tumor
Plasma cell	CD138	Produce antibody
Macrophage	CD68	Assist T cell and kill tumor
Naïve/Effecter T cell	CD45RA+	Naïve/Effecter T cell
Memory T cell	CD45RO (RA-)	Antigen committed T cell

**[0125]** The presence of IHC stained markers was evaluated under low power and graded using a prospectively defined 0-100 mm visual analog scale (VAS), where 0 represented 0% presence and 100 represented 100% of cells staining positive for the marker. The peroxidase reaction used to highlight the marker overestimates the area or density of lymphocyte infiltration as compared to H&E staining, thus making IHC-based density determinations unreliable, but IHC remains useful for elucidating the relative relationships between and among cell types.

#### **H&S Studies: Methods and Analyses**

**[0126]** Three analyses were performed comparing the H&E stained slides. Two analyses were blinded feature extractions from the 25 IRX-2 treated and 25 untreated surgical specimens from MD Anderson, one for tumor features and one for immune response features. The third analysis was an identical but unblended immune response feature extraction from the 10 H&E stained slides from Stony Brook. In each case, features were extracted and quantified using a VAS on case report forms.

**[0127]** Two assessments were made for each of the immune response features, the first assessment was the overall presence of the marker across the entire surgical specimen and

the second was to the degree to which the location of the infiltrate was peripheral or intratumoral.

**[0128]** An overall assessment was made taking into account: lymphocyte infiltration, its density, its balance between tumor and infiltration, and other features that comprise the gestalt impression of the tumor. The other sub-features include the extent of fibrosis and necrosis, suggesting where tumor was but is no longer and in the case of well differentiated squamous cell cancer, a concentration of keratin pearls with minimal or no tumor surrounding it is another sign of tumor destruction. An "Active Immunologic Response" includes lymphoid infiltration evidence of damage created by the immune system, and the degree to which tumor is no longer viable and disrupted - in short the extent and process by which the host is combating the tumor. An example of the lymphocyte infiltration sub-feature of the "Active Immune Response" is presented in FIGURES 19 and 20.

**[0129]** One of the dominant sub-features on the Active Immune Response variable is the localization and intensity of the lymphocyte infiltration (LI) that are observed in patients treated with IRX-2. Surgical specimens demonstrating this reaction in both IRX-2-treated patients and the ad-hoc comparator groups demonstrated marked increases in the density of overall LI, peritumoral LI, and intratumoral LI.

**[0130]** Based on the pre-specified critical point of 50 mm or greater on the VAS, the analysis showed different Active Immunologic Response rates among the three groups of surgical specimens as showed in Table 9 below.

**TABLE 9**

Group	Patient w/AIR	Total Patients	Active Immune Response Rate
1. IRX-2 Treated	11	25	44.0%
2. MD Anderson	6	1	24.0%
3. Stony Brook	1	10	10.0%

**[0131]** The increase in the frequency of those patients demonstrating an Active Immune Response went from 20% in the pooled MD Anderson and Stony Brook groups to 44% in the IRX-2 treated group ( $p < 0.05$  by Chi square test).

#### Determination of Peritumoral vs. Intratumoral LI

**[0132]** The location of immune cells in the tumor was also evaluated. It was hypothesized herein that an active anti-tumor immune response would include lymphocytic infiltrate that expanded from the peripheral area to include the intratumoral area.

**[0133]** Based upon the VAS analysis for Active Immune Response in the IRX-treated patients,

11 showed intense reactions  $\geq 50$ , termed responders) and 14 showed less intense reactions ( $< 50$ , termed non-responders). A comparison of the LI of these two groups is shown in FIGURES 21A and 21B.

**[0134]** As can be seen, the responders showed a marked increase in LI (both area and density) of the typical section and compared to the non-responders, the increase in intratumoral LI is proportionally much greater than the peritumoral change.

**[0135]** Immunohistochemistry for the location of various markers helps clarify which cells dominate in each region. FIGURE 22 shows these results. The peritumoral infiltrate, representing approximately 25% of the LI in the specimen was dominated by CD45RA+, CD3+, CD4+ T lymphocytes and CD20+ B lymphocytes. Whereas the intratumoral infiltrate, representing approximately 75% of the LI in the specimen, was dominated by CD45RO+, CD3+ and CD8+ lymphocytes (i.e. the "killer" effector T cell phenotype) and CD68+ macrophages. FIGURE 23 provides a pictoral example of IHC staining fro CD45RO+ memory T cells in an IRX-2 treated surgical specimen. TABLE 10 shows the results of each cell population's presence in the tumor.

TABLE 10

Cell Population	N	Presence in the Tumor*	
		Overall Mean	Intratumoral Mean
T cell (CD3)	24	52.3	76.5
B cell (CD20)	24	11.0	21.2
Helper T cell (CD4)	24	15.5	53.1
Cytotoxic T cell (CD8)	24	37.8	85.7
Macrophage (CD68)	24	42.1	91.5
Effector T cell (CD45 RA)	24	7.4	18.4
Memory T cell (CD45 RO)	24	65.4	87.3

\*Measurements based on 100 mm Visual Analog Scale (VAS) assessments

**[0136]** The strongest support for this immunization hypothesis derives from the examination of lymphocyte infiltration for infiltration in and around the tumor and the picture of tumor rejection indicating necrosis, fibrosis, and reduced tumor. The rejection patterns are characteristic for both humoral and cellular immunity with increased B lymphocytes and activated macrophages within the tumor, respectively. By shifting the balance back to immunosurveillance by overcoming the immune suppression seen in cancer patients and restoring immune function, IRX-2 therapy causes the host to reject the tumor and immunize itself against the tumor leading to reduced recurrence and increased survival.

#### EXAMPLE 13 (not according to the invention)

**[0137]** In one patient, fused FDG PET/CT scans were compared at day 0 and day 21, as shown in FIGURE 24. Total glycolytic activity and volume were measured and are shown in Table 11.

**TABLE 11**

<u>Total Glycolytic Activity</u>			
	<u>Baseline</u>	<u>Day 21</u>	<u>% Change</u>
Tumor	68.91	31.36	-54.49%
Node 1	72.54	4.97	-93.15%
Node 2	14.35	3.15	-78.05%
	155.80	39.48	-74.66%
<u>Volume</u>			
	<u>Baseline</u>	<u>Day 21</u>	<u>% Change</u>
Tumor	12.16	7.33	-39.72%
Node 1	9.46	1.44	-84.78%
Node 2	2.28	1.24	-45.61%
	23.90	10.01	-58.12%

**EXAMPLE 14 (not according to the invention)**

**[0138]** Overall survival was determined both for patients overall (FIGURE 25) and for patients in Stage IVa (FIGURE 26). FIGURE 25 shows three Kaplan Meir plots of overall survival. The top line is the recently completed multicenter Phase 2 study (median follow-up of 18.6 months), the middle line is the single center Phase 1/2 study completed 10 years ago and as compared to the best available comparator-the randomized site matched RTOG 9501 trial. In both IRX-2 treated groups, survival is above the anatomic site-matched RTOG 9501 trial data. The data suggests that the IRX-2 driven immunization is durable and leads to improved survival. Figure 26 shows the three Kaplan Meier plots of overall survival the Stage Iva cohort. The top line is the recently completed multicenter Phase 2 study (median follow-up of 18.6 months), the middle line is the single center Phase 1/2 study completed 10 years ago and as compared to the best available comparator-the randomized site matched RTOG 9501 trial. In both IRX-2 treated groups, survival is above the anatomic site-matched RTOG 9501 trial data. The data suggests that the IRX-2 driven immunization is durable and leads to improved survival in Stage IVa patients.

**EXAMPLE 15 (not according to the invention)**

**[0139]** IRX-2 was shown to increase regional lymph node size, T cell area and density, and reverse sinus histiocytosis. Controls, H&NSCC controls, and H&NSCC patients administered IRX-2 are compared in FIGURES 27A-D. Twenty patients from a total of 50 with H&N SCC treated with the IRX-2 protocol were selected as having uninvolving regional lymph nodes suitable for evaluation. All displayed clinical responses, either partial responses (PR, >50% tumor reduction) or minor responses (MR, < 50% >25% tumor reduction). Complete responders (3/50) and non-responders (5/50) were excluded for obvious reasons. Ten untreated H&N SCC control LN specimens were selected randomly as one control group (H&N SCC control) and 10 non-cancer control LN biopsies were selected randomly (control group). Obvious LN pathologies were excluded from the control group. Overall, 95% of the IRX-2 LN, 80% of the noncancer controls, and 60% of the H&N SCC controls were adjudged to be stimulated. Overall, the LN of IRX-2-treated patients showed a high percentage of stimulation with a shift toward T cell reactivity. The mean size of the LN of H&N SCC controls was significantly smaller than the control group and those of the IRX-2-treated H&N SCC patients were significantly larger than both cancer and non-cancer control (p's < 0.01) (FIGURE 27A). The non-T and B cell "other cell" LN area by subtraction and by PAS staining was approximately 25% of the total and corresponded mostly to the degree of sinus histiocytosis (Fig. 5). It is of note that sinus histiocytosis was marked in the H&N SCC control but not in the other groups. In 9 of the 10 H&N SCC controls, but in none of the other cases, sinus congestion with erythrocytes was also observed; however, erythrophagocytosis by the histiocytes, either B and PC or T lymphocytes, were calculated and correlated with the area of the lymph node bearing the corresponding lymphoid populations. (FIGURE 27C). The T cell area of H&N SCC controls was modestly reduced (p = NS) and the density significantly reduced (p < 0.01), compared to non-cancer controls (FIGURE 27B). T cell area of IRX-2-treated patients was modestly increased compared to non-cancer controls (p = NS) and significantly so over the H&N SCC controls (p < 0.01). T cell density of the IRX-2-treated LN was significantly greater than both controls (p's <0.01) FIGURE 27D.

#### **EXAMPLE 16 (not according to the invention)**

**[0140]** FIGURES 28A-D - Sinus histiocytosis is characterized by the majority of cells being large, granular, PAS-positive and a minority of CD3+T cells of varying size. FIGURE 28A depicts a typical example of a HN SCC control with Sinus Histiocytosis. FIGURE 28B shows CD68+ staining of a lymph node with Sinus Treatment with IRX-2 was associated with a reversal of sinus histiocytosis apparent in the HN SCC controls. FIGURE 28C shows a typical example of a lymph node with sinus histiocytosis and erythrocyte congestion. FIGURE 28D is a bar graph showing the reversal of sinus histiocytosis in IRX-2 treated patients.

#### **EXAMPLE 17 (not according to the invention)**

**[0141]** FIGURES 29A-F - The upper panel shows examples of the pre-treatment biopsy of

three patients with squamous cell head and neck cancer (H&N SCC). The biopsies average 80% tumor and 20% stroma with a light sprinkling of lymphocytes in the stroma. The lower panel shows typical sections of the tumor following treatment with the IRX-2 regimen. Notable is the heavy infiltration of lymphocytes with displacement of tumor. In this trial at INCAN 22/25 patients (88%) showed the response.

**EXAMPLE 18 (not according to the invention)**

**[0142]** FIGURE 30 Shows the intensity of necrosis and fibrosis in the surgical specimen of 11 responder patients (44%) vs 14 non- responder patients treated with the IRX-2 regimen in the US Phase 2 trial.

**EXAMPLE 19 (not according to the invention)**

**[0143]** IRX-2 is shown to stimulate killer T cell infiltration that causes tumor destruction, as shown in FIGURES 31A-D. FIGURES 31A-D are H&E and IHC (Immunohistochemistry) stains of resection specimens from patients treated with IRX-2. Despite the heterogeneity of tumors, there is seen an increased frequency of the brisk infiltrate pictured in FIGURE 31B and noted by the arrow as a lake of lymphocytes. Pictured in FIGURE 31D, the immunohistochemistry staining confirms that the infiltrate is the CD45RO memory killer T-cell phenotype. There is growing evidence that lymphocyte infiltration into tumors predicts improved outcome in colorectal, ovarian, breast, head and neck cancer. The lymphocytic infiltrate provides a link as to why patients appear to be living longer without disease than expected - the result of immune memory that can attack micro metastases and thereby delay or prevent recurrence and improve survival.

**EXAMPLE 20 (not according to the invention)**

**[0144]** Immunohistochemistry was performed to compare intratumoral versus peritumoral infiltrates. Summary data from the evaluation of overall presence and location of immune cells in the tumor resection specimen based on immunohistochemistry stain is presented below in Table 12. The combined presence of B cells in the tumor's peripheral area and the diffuse intratumoral lymphocytic infiltrate that is primarily CD8+ and CD45 RO+ (ie, the "killer" effector T-cell phenotype) copresent with activated CD68+ macrophages suggest antigenic stimulation and an antitumor immune response.

TABLE 12

	Responders	Non-Responders	P value
CD3	85:15	69:31	< 0.05
CD4	59:41	49:51	NS

	Responders	Non-Responders	P value
CD8	93:7	80:20	< 0.05
CD45RO	97:3	79:21	< 0.01
CD45RA	32:68	2:98	< 0.02
CD20	30:70	17:83	NS
CD68	96:4	88:12	< 0.01

#### EXAMPLE 21 (not according to the invention)

##### Dendritic cells

**[0145]** One of the key cell types that IRX-2 acts on is the dendritic cell. Cancer patients have reduced dendritic cell function as a result of reduced antigen uptake, antigen presentation, and expression of the signaling molecules necessary for effective T cell stimulation.

**[0146]** As shown in FIGURE 32, the key signaling molecules for T cell stimulation and adhesion on dendritic cells are CD86, CD40 and CD54. In cancer patients, the components of the antigen presenting machinery are down-regulated in dendritic cells, resulting in a reduction of effective antigen presentation to T cells. IRX-2 is able to activate and mature dendritic cells both phenotypically and functionally. By increasing expression of the antigen presenting machinery, IRX-2 acts to restore antigen presentation function.

**[0147]** Shown in FIGURE 33 is highly statistically significant flow cytometry data that show the actions of IRX-2 on the dendritic cell's antigen presenting machinery and T cell stimulatory capacity. HLA-DR up-regulation is required by dendritic cells to present antigen in the MHC Class II groove. CD86 is the co-stimulatory receptor for naïve T-cells, that is one of the required signals for T-cell activation and the creation of killer memory T-cells. Dendritic cells that do not express CD86 are tolerizing dendritic cells and function to create antigen-specific suppressive regulatory T cells. By administering IRX-2 and increasing the co-stimulatory proteins, it is possible to shift this balance from tolerizing dendritic cells to activating dendritic cells, and a coordinated and robust immune response against the immune target is initiated.

**[0148]** FIGURE 34 shows highly statistically significant flow cytometry data that show the actions of IRX-2 on the dendritic cells' potential T cell stimulatory capacity. Increases in CD40 expression are necessary to generate a sustained T cell activation and generation of memory T cells. CD54 also called ICAM-1, and is involved in dendritic cell-T cell interactions and provides a second of the required signals for T-cell activation. Thus the up-regulation of these molecules in dendritic cells ensures that the cellular immune response initiated by IRX-2 is sustained and robust.

**[0149]** FIGURE 45 shows data comparing various dilutions of IRX-2 and recombinant TNF and their respective ability to up-regulate CD83 expression, a marker of mature dendritic cells. The multiple active components in IRX-2, present in physiologic quantities, act synergistically to increase CD83 expression by about 4 times the magnitude of the equivalent amount of TNF present in IRX-2. To achieve similar results with TNF alone, 10-25 times the concentration was required, amounts that would clearly exceed the concentration in tissue or lymph node (supra-physiologic/pharmacologic).

**[0150]** FIGURE 36 shows data from an assay to determine the ability of dendritic cell to induce T-cell proliferation, a functional assessment of a dendritic cell's ability to activate naïve T-cells. IRX-2 enhances T cell stimulatory activity of DC. Immature DC (GM-CSF/IL4 x 7d) were stimulated with IRX-2 or X-VIVO 10 media alone control (closed or open circles, respectively). After 48h, DC were harvested, washed extensively and co-cultured with allogeneic nylon wool-purified T cells (2 x 10<sup>5</sup>/ well) in round bottom 96-well microtiter plates at the indicated stimulator (DC) to responder (T) ratios. On day 5 of the co-culture, cells were pulsed with BrdU and incorporated BrdU was measured 18h later by a colorimetric anti-BrdU ELISA assay. This graph shows the results from a representative donor of 6 individual donors tested, expressed as mean stimulation index (S.I.) (+/- SEM) at the 4 DC:T ratios tested. S.I. is defined as [(O.D. DC stimulated T cell - O.D. DC alone)/O.D. resting T cell]. The mean S.I. from all 6 donors across the entire range of DC:T ratios showed a statistically significant improvement when IRX-2-treated DC were used as stimulators ( $p<0.05$ , by ANOVA).. There was a significant increase in the IRX-2 treated dendritic cells ability to induce T-cell proliferation - a confirmation that the phenotypic dendritic cell changes induced by IRX-2 also results in a functionally active dendritic cell that is capable of effectively causing T cell stimulation and proliferation.

#### **EXAMPLE 22 (not according to the invention)**

#### **IRX-2 enhances peptide-specific IFN- $\gamma$ production and DTH**

**[0151]** Mice were immunized with varying doses of PSMA peptides with and without IRX-2. The T cell response after peptide or conjugate challenge was assessed by DTH response (FIGURE 37A) or IFN- $\gamma$  production (FIGURE 37B) in response to a subsequent peptide. IRX-2 plus conjugate vaccine enhances antigen specific cellular T cell response *in vivo* (DTH) and *ex vivo* (IFN- $\gamma$  production by spleen lymphocytes). This is important because a cellular response is an essential requirement in an effective cancer vaccine. Also, the T cell responses *in vivo* and *ex vivo* are both related to the dose of the vaccine used with IRX-2. The dose response confirms that the response is vaccine antigen driven and not just due to IRX-2.

#### **EXAMPLE 23 (not according to the invention)**

**IRX-2 is superior to other adjuvants in enhancing peptide-specific DTH**

**[0152]** The novel nature of the IRX-2 activity was confirmed by comparing IRX-2 to other adjuvants which were selected to represent various mechanisms of action. Alum was evaluated because it is a widely used FDA approved adjuvant, CpG because it is a TLR agonist that targets antigen presenting cells and the RIBI Adjuvant System (RAS) because it contains multiple adjuvant activities and is a safer alternative than Freund's adjuvant. As shown in FIGURE 38 all of the adjuvants tested caused a DTH response when challenged with the conjugate; however, only IRX-2 enhanced the peptide-specific DTH response to the conjugate vaccine while alum, CpG or RAS did not as shown in FIGURE 43. The studies reported here provide important preclinical data supporting the hypothesis that IRX-2 enhances T cell immune responses to exogenous antigens for use in combination with multiple antigen types in therapeutic cancer vaccines. The unique nature of the T cell peptide-specific response to the conjugate vaccine is a result of the multi-target mode of action of IRX-2 and the presumed synergy among the cytokines.

**EXAMPLE 24 (not according to the invention)****Evidence of action on immune cells in peripheral circulation**

**[0153]** The following data are summarized from immune monitoring of peripheral blood at baseline and day 21. Statistically significant decreases in peripheral blood in 21 days in the CCR7<sup>+</sup> cell populations-those with lymph node homing potential and B cells are consistent with these cells recruitment out of the circulation and into lymph nodes for activation by dendritic cells. No change or a slight trend towards increased numbers of effector cells are consistent with cytotoxic T cells that pass temporarily into the circulation and then into tissue to kill the antigenic target. The overall changes in peripheral blood of the IRX-2 regimen treated patients of both immune cells and T regulatory cells are consistent with an immunization in lymph nodes a shift from a tolerizing to a stimulating environment, as shown generally in FIGURE 39.

**[0154]** Presented in FIGURE 40 are the absolute counts at baseline and day 21 (after completion of IRX-2 regimen) of T regulatory cells in peripheral blood from Head and Neck cancer patients. Each line represents a patient and the bold line represents the group mean. Several prior studies have indicated that T reg cells are increased in cancer patients (ovarian, colorectal, hepatocellular, HNSCC) and that increased T reg is associated with a worse prognosis. The fact that the T reg of 18 of 26 patients stay the same or go down in only 21 days is a striking and significant finding because tolerizing dendritic cells should continue to expand the T reg population. The IRX-2 regimen stabilizes Treg counts at baseline levels is a

significant finding reflective of improved survival in these patients.

**EXAMPLE 25 (not according to the invention)**

**Evidence of tumor shrinkage consistent with immunization**

**[0155]** FIGURE 41A and 41B show fused FDG-PET / CT scans of a large 5.2 cm right base of tongue primary with two involved lymph nodes shows a 58% reduction in volume and a 75% reduction in total glycolytic activity in 21 days. There is evidence of tumor shrinkage which supports the hypothesis that an anti-tumor rejection and immunization is occurring.

**EXAMPLE 26 (not according to the invention)**

**[0156]** Previously, the criteria for histopathology of a biopsy versus a tumor specimen (Meneses) were that the tumor was reduced overall, fragmentation of the tumor occurred, and there was increased lymphocyte infiltration (LI). According to the present invention, there are new criteria presented herein for a treated tumor versus a control tumor, namely tumor disruption with necrosis and fibrosis, and increased LI that is greater intratumorally than peritumorally. Table 13 below summarizes various findings of cytokine treatment on H&NSCC. Importantly, IRX-2 is shown to work on all arms of the immune system whereas other multiple component cytokine therapeutics do not. MULTIKINE (Cel-Sci) includes multiple cytokines in its formulation; however, its effect is a single one on the tumor itself, not on the immune system.

**TABLE 13**

	Treated	Control	
De Stefani rIL-2	Tumor	Control tumor	↑ LI, ↑ necrosis, ↑ fibrosis
Meneses IRX-2	Tumor	Biopsy	↑ LI, ↓ tumor, ↑fragmentation
Feinmesser Multikine	Tumor	Biopsy	↑ LI, ↓ tumor
Timar Multikine	Tumor	Control tumor	↑ LI, No ↓ tumor or fragmentation
IRX Therapeutics	Tumor	Biopsy	↑ LI - small tumor, ↑fragmentation
	Tumor	Control tumor	↑ LI, ↑ fibrosis

**OVERALL CONCLUSION**

**[0157]** This study confirms and extends Applicants' prior observations concerning the ability of

the IRX-2 regimen to have significant biological activity on patients with squamous cell head and neck cancer treatment prior to surgery. The present study confirms that the treatment is safe with few adverse events attributed to the regimen. In fact, those patients who showed evidence of histopathologic changes of lymphocyte infiltration had the majority of symptom improvements like reduced pain and tenderness, improved breathing and phonation, and softening of the tumor (as sign of dissolution). Three patients were adjudged to have clinical responses (2PRs, 1 MR). Overall survival data and recurrence free survival while immature are encouraging and similar in degree and profile to Applicants' previous study. Notable is that no deaths occurred due to recurrence in the first 12 months of follow up. All deaths to date but one are in the non-responder group.

**[0158]** The most compelling data are those associated with the mechanism of action studies. It was observed that declines of B lymphocytes and two T cell subsets associated with initial immunization and lymph node homing. No increases in memory/effector cell were observed in blood; however, this is explainable based upon the traffic patterns of T cells which occur with an immunization. Notably no increase in T regs was observed.

**[0159]** Applicants' prior studies showed that patients responding to the IRX-2 regimen show increase of uninvolved lymph nodes proximal to the tumor, replenishment of depleted T lymphocyte areas and the picture of activation as occurs with antigen. Thus, lymphocytes are trafficking via blood and lymphatics to the regional lymph nodes where they are presumably immunized to autologous tumor antigens. As shown herein, they then leave the lymph node and travel by blood to the tumor where they infiltrate in and around the tumor and correlate with evidence of tumor destruction (necrosis, fibrosis, and tumor reduction). In the patients showing this reaction, the increases in lymphocyte infiltration involves predominantly CD3+ CD4+ CD45RA+ T cell populations and CD20+ B lymphocytes around the tumor periphery and CD3+ CD8+ CD45RO+ T lymphocyte populations and macrophages within the tumor. The changes within the tumor are greater than these in the periphery. This mechanism is generally shown in FIGURE 2.

**[0160]** Notably, untreated patients show such a reaction only occasionally (20%) and while significantly less frequently than patients treated with the IRX-2 regimen (44% vs. 20%) the presence of the reaction in controls represent a new biomarker for predicting favorable outcome.

**[0161]** The picture is an integrated one clinically, radiologically, pathologically, and immunologically and provides ample evidence for an immunization to autologous tumor antigen. IRX-2 is shown to activate all arms of the immune system to provide a total restoration of immune function and ability to attack immune targets.

**[0162]** The invention has been described in an illustrative manner, and it is to be understood that the terminology which has been used is intended to be in the nature of words of description rather than of limitation.

**[0163]** Obviously, many modifications and variations of the present invention are possible in light of the above teachings. It is, therefore, to be understood that within the scope of the appended claims, the invention may be practiced otherwise than as specifically described.

## REFERENCES

### [0164]

Dunn G, et al. Dendritic cells and HNSCC: A potential treatment option? (Review). *Oncology Reports* 13:3-10, 2005.

Egan JE, et al. IRX-2, a novel *in vivo* immunotherapeutic, induces maturation and activation of human dendritic cells *in vitro*. *J Immunother* 30:624-633, 2007.

Galon J, et al. Type, density, and location of immune cells within human colorectal tumors predict clinical outcome. *Science* 313:1960, 2006.

Hadden JW, et al. Immunotherapy with natural interleukins and/or thymosin alpha 1, potently augments T-lymphocyte responses of hydrocortisone-treated aged mice. *Int J Immunopharm* 17(10):821-828, 1995.

Hadden JW, et al. Zinc induces thymulin secretion from human thymic epithelial cells *in vitro* and augments splenocytes and thymocyte responses *in vivo*. *Int J. Immunopharm* 17(9):729-733, 1995.

Kaech SM, et al. Effector and memory T-cell differentiation: implications for vaccine development. *Nature Rev Immunol* 2:251, 2001.

Lanzavecchia A, et al. Understanding the generation and function of memory T cell subsets. *Curr Opin Immunol* 17:326, 2005.

Maass G, et al. Priming of tumor-specific T cells in the draining lymph nodes after immunization with interleukin-2-secreting tumor cells: Three consecutive stages may be required for successful tumor vaccination. *Proc Natl Acad Sci* 92:5540, 1995.

Mantovani A, et al. Macrophage polarization: tumor associated macrophages as a paradigm for polarized M2 mononuclear phagocytes. *Trends in Immunology*, 23 (11) 2002.

Meneses A, et al. Lymph node histology in head and neck cancer: impact of immunotherapy with IRX-2. *Int'l Immunopharm*. 3:1083-1091, 2003.

Pages F, et al. Effector memory T cells, early metastasis, and survival in colorectal cancer. *NEJM* 353:2654-66, 2005.

Sallusto F, et al. Two subsets of memory T lymphocytes with distinct homing potentials and effector functions. *Nature* 401:708, 1999.

Tomiyama H, et al. Phenotypic classification of human CD8+ T cells reflecting their function: inverse correlation between quantitative expression of CD27 and cytotoxic effector function. Eur J Immunol 34:999, 2004.

Verastegui E, et al. Immunological approach in the evaluation of regional lymph nodes of patients with squamous cell carcinoma of the head and neck. Clin Immunol 102:37, 2002.

Whiteside TL. Immunobiology and immunotherapy of head and neck cancer. Curr Onc Reports 3:46-55, 2001.

Wolf GT, et al. Lymphocyte subpopulations infiltration squamous carcinomas of the head and neck: correlations with extent and tumor prognosis. Otolaryngol Head Neck Surg 95:145, 1986.

## REFERENCES CITED IN THE DESCRIPTION

This list of references cited by the applicant is for the reader's convenience only. It does not form part of the European patent document. Even though great care has been taken in compiling the references, errors or omissions cannot be excluded and the EPO disclaims all liability in this regard.

### Patent documents cited in the description

- [US990759P \[0014\]](#)
- [US6977072B \[0015\] \[0038\] \[0049\]](#)
- [US7153499B \[0015\] \[0038\] \[0049\]](#)
- [WO2006039545A \[0021\]](#)
- [WO2005056041A \[0022\]](#)
- [WO2007060524A \[0023\]](#)
- [US61044674A \[0040\] \[0062\]](#)

### Non-patent literature cited in the description

- **DUNN G et al.** Dendritic cells and HNSCC: A potential treatment option? Oncology Reports, 2005, vol. 13, 3-10 [\[0164\]](#)
- **EGAN JE et al.** IRX-2, a novel *in vivo* immunotherapeutic, induces maturation and activation of human dendritic cells *in vitro*. J Immunother, 2007, vol. 30, 624-633 [\[0164\]](#)

- **GALON J et al.** Type, density, and location of immune cells within human colorectal tumors predict clinical outcome *Science*, 2006, vol. 313, 1960- [\[0164\]](#)
- **HADDEN JW et al.** Immunotherapy with natural interleukins and/or thymosin alpha 1, potently augments T-lymphocyte responses of hydrocortisone-treated aged mice *Int J Immunopharmac*, 1995, vol. 17, 10821-828 [\[0164\]](#)
- **HADDEN JW et al.** Zinc induces thymulin secretion from human thymic epithelial cells in vitro and augments splenocytes and thymocyte responses in vivo *Int J. Immunopharmac*, 1995, vol. 17, 9729-733 [\[0164\]](#)
- **KAECH SM et al.** Effector and memory T-cell differentiation: implications for vaccine development *Nature Rev Immunol*, 2001, vol. 2, 251- [\[0164\]](#)
- **LANZAVECCHIA A et al.** Understanding the generation and function of memory T cell subsets *Curr Opin Immunol*, 2005, vol. 17, 326- [\[0164\]](#)
- **MAASS G et al.** Priming of tumor-specific T cells in the draining lymph nodes after immunization with interleukin-2-secreting tumor cells: Three consecutive stages may be required for successful tumor vaccination *Proc Natl Acad Sci*, 1995, vol. 92, 5540- [\[0164\]](#)
- **MANTOVANI A et al.** Macrophage polarization: tumor associated macrophages as a paradigm for polarized M2 mononuclear phagocytes *Trends in Immunology*, 2002, vol. 23, 11 [\[0164\]](#)
- **MENESES A et al.** Lymph node histology in head and neck cancer: impact of immunotherapy with IRX-2 *Int'l Immunopharmac*, 2003, vol. 3, 1083-1091 [\[0164\]](#)
- **PAGES F et al.** Effector memory T cells, early metastasis, and survival in colorectal cancer *NEJM*, 2005, vol. 353, 2654-66 [\[0164\]](#)
- **SALLUSTO F et al.** Two subsets of memory T lymphocytes with distinct homing potentials and effector functions *Nature*, 1999, vol. 401, 708- [\[0164\]](#)
- **TOMIYAMA H et al.** Phenotypic classification of human CD8+ T cells reflecting their function: inverse correlation between quantitative expression of CD27 and cytotoxic effector function *Eur J Immunol*, 2004, vol. 34, 999- [\[0164\]](#)
- **VERASTEGUI E et al.** Immunological approach in the evaluation of regional lymph nodes of patients with squamous cell carcinoma of the head and neck *Clin Immunol*, 2002, vol. 102, 37- [\[0164\]](#)
- **WHITESIDE TL** Immunobiology and immunotherapy of head and neck cancer *Curr Onc Reports*, 2001, vol. 3, 46-55 [\[0164\]](#)
- **WOLF GT et al.** Lymphocyte subpopulations infiltration squamous carcinomas of the head and neck: correlations with extent and tumor prognosis *Otolaryngol Head Neck Surg*, 1986, vol. 95, 145- [\[0164\]](#)

## Patentkrav

1. Anvendelse af et naturligt primært celleafledt biologisk lægemiddel, der omfatter interleukin-1 $\beta$  (IL-1 $\beta$ ), interleukin-2 (IL-2), interleukin-6 (IL-6), interleukin-8 (IL-8), tumornekrosefaktor- $\alpha$  (TNF- $\alpha$ ) og  $\gamma$ -interferon (IFN- $\gamma$ ), til forlængelse af levetiden for T-celler *in vitro*.  
5
2. Anvendelse ifølge krav 1, hvor det naturlige primære celleafledte biologiske lægemiddel omfatter 60-6.000 pg/ml IL-1 $\beta$ , 600-60.000 pg/ml IL-2, 60-6.000 pg/ml IL-6, 6000-600.000 pg/ml IL-8, 200-200.000 pg/ml TNF- $\alpha$  og 200-200.000 pg/ml IFN- $\gamma$ .  
10
3. Anvendelse ifølge krav 2, hvor det naturlige primære celleafledte biologiske lægemiddel omfatter 150-1.800 pg/ml IL-1 $\beta$ , 3.000-12.000 pg/ml IL-2, 300-2.000 pg/ml IL-6, 20.000-180.000 pg/ml IL-8, 1.000-4.000 pg/ml TNF- $\alpha$  og 1.000-4.000 pg/ml IFN- $\gamma$ .  
15
4. Anvendelse ifølge krav 1, hvor det naturlige primære celleafledte biologiske lægemiddel er dannet af oprensede humane hvide blodlegemer stimuleret med et mitogen og ciprofloxacin.  
20
5. Anvendelse ifølge krav 4, hvor mitogenet er phytohæmagluttinin.  
25
6. Anvendelse ifølge krav 1, hvor det naturlige primære celleafledte biologiske lægemiddel kan opnås ved hjælp af oprensede humane hvide blodlegemer ved vedvarende tilstedeværelse af 4-aminoquinolon-antibiotikum og ved vedvarende eller pulseret tilstedeværelse af et mitogen.  
30
7. Anvendelse ifølge et hvilket som helst af ovennævnte krav, hvor T-cellerne er CD4- eller CD8-positive.  
35

## DRAWINGS

Figure 1

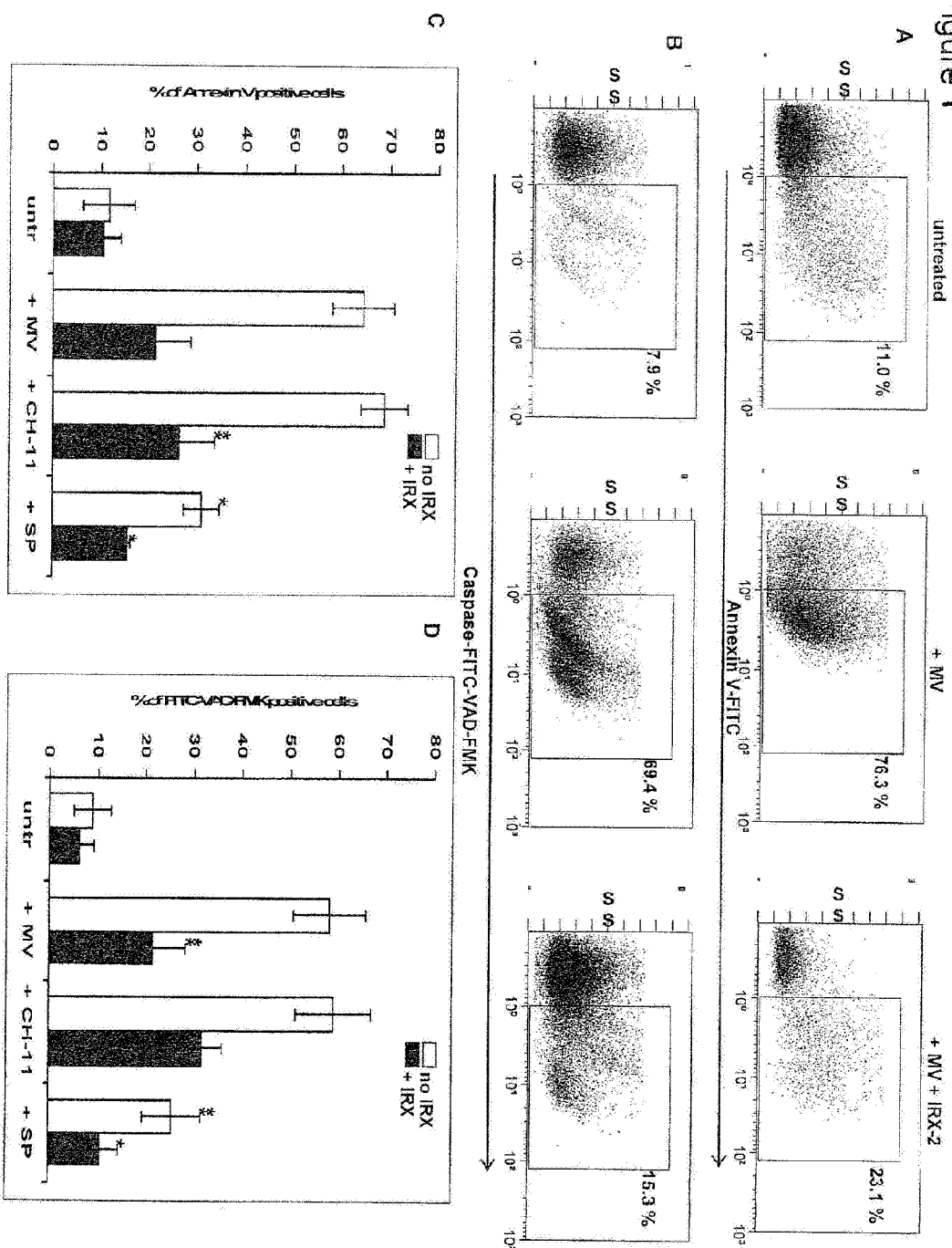


Figure 2

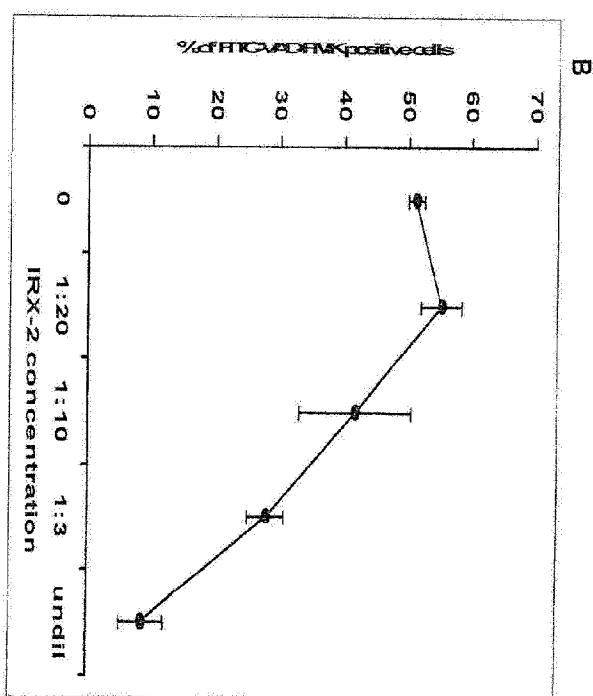
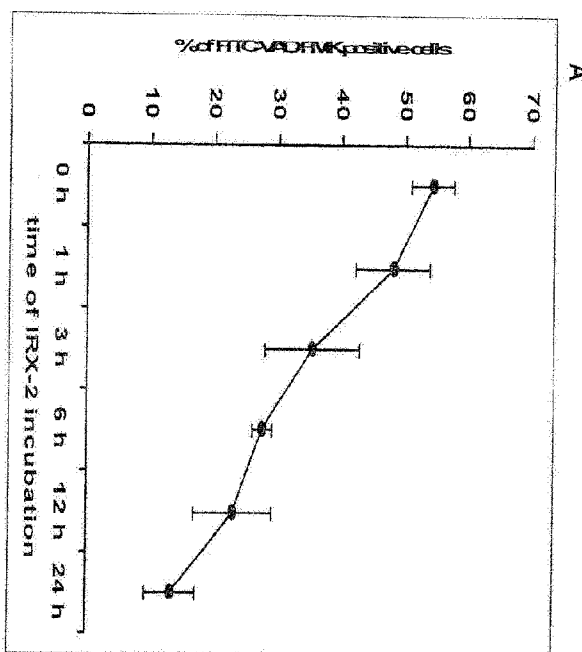


Figure 3

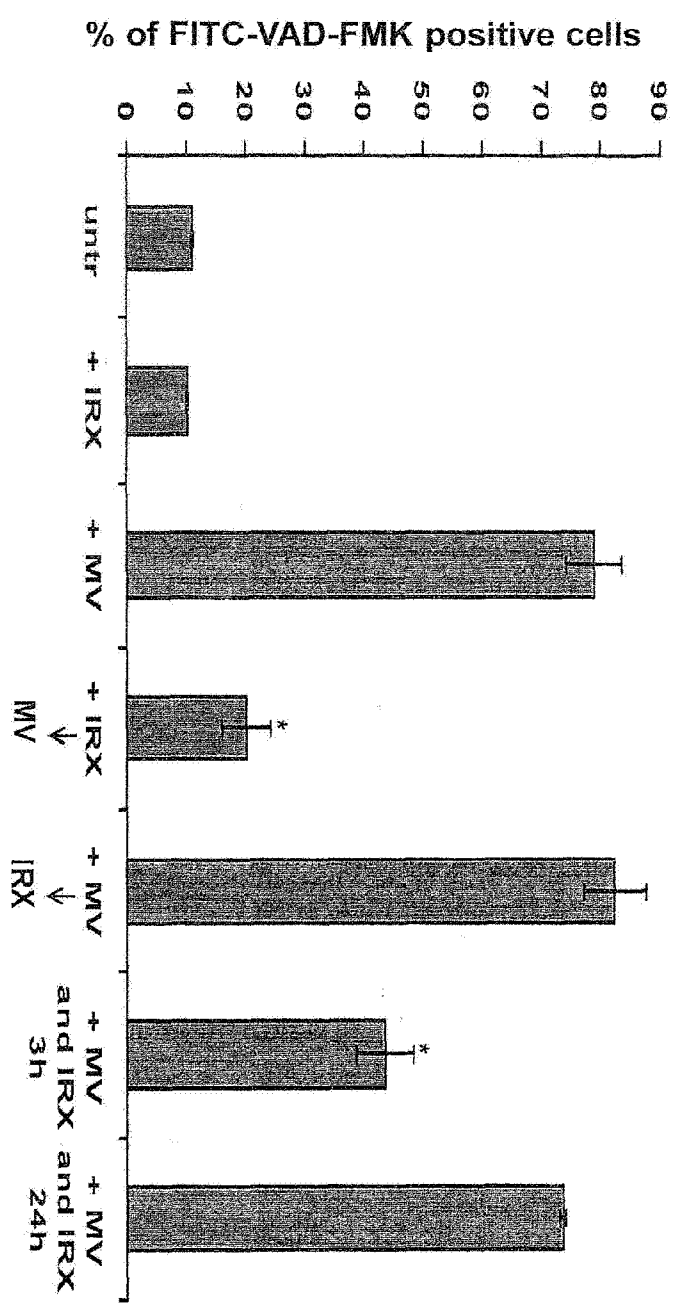
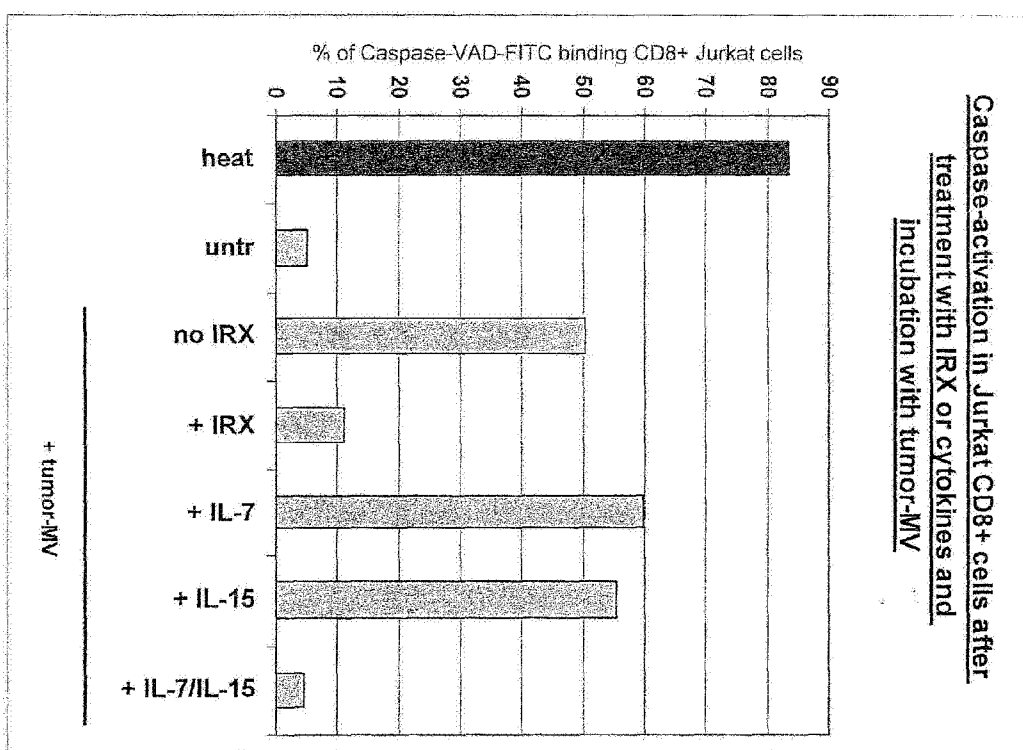


Figure 4



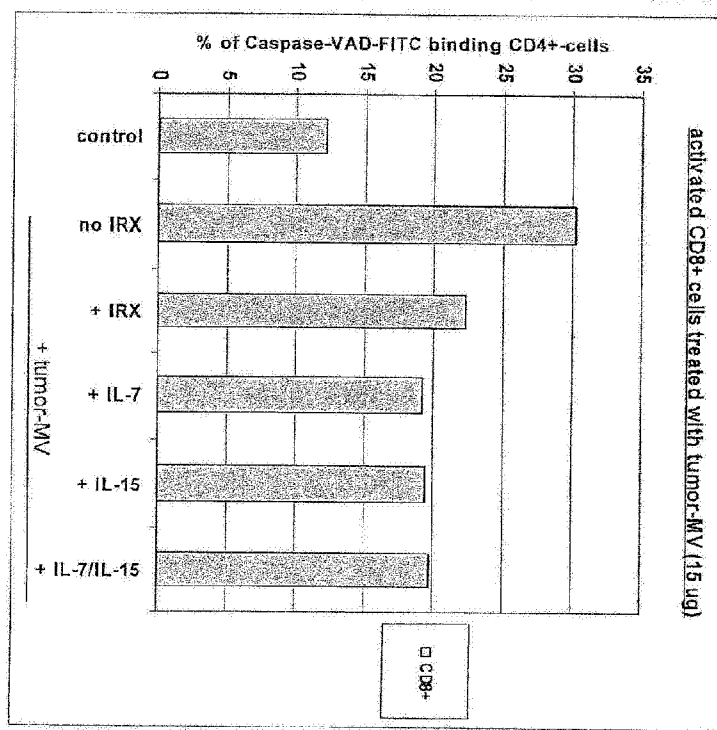
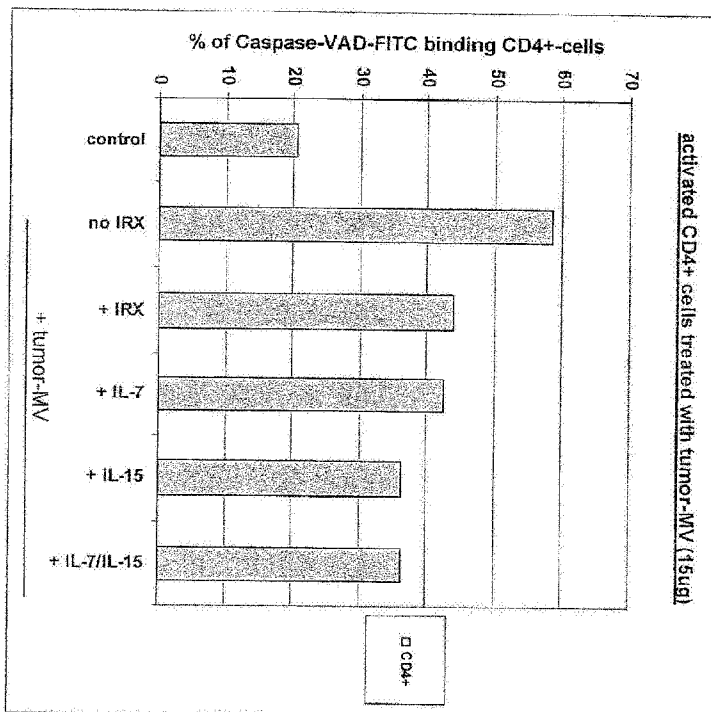


Figure 6A

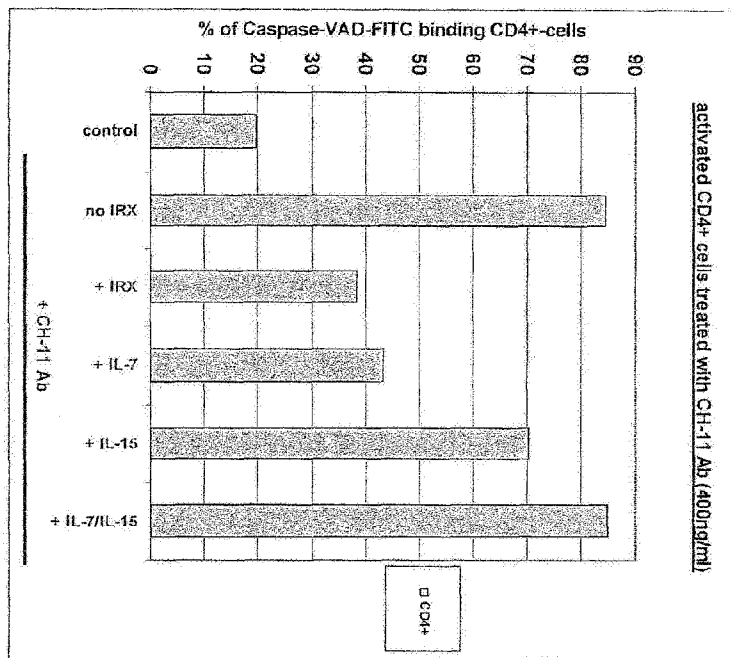


Figure 6B

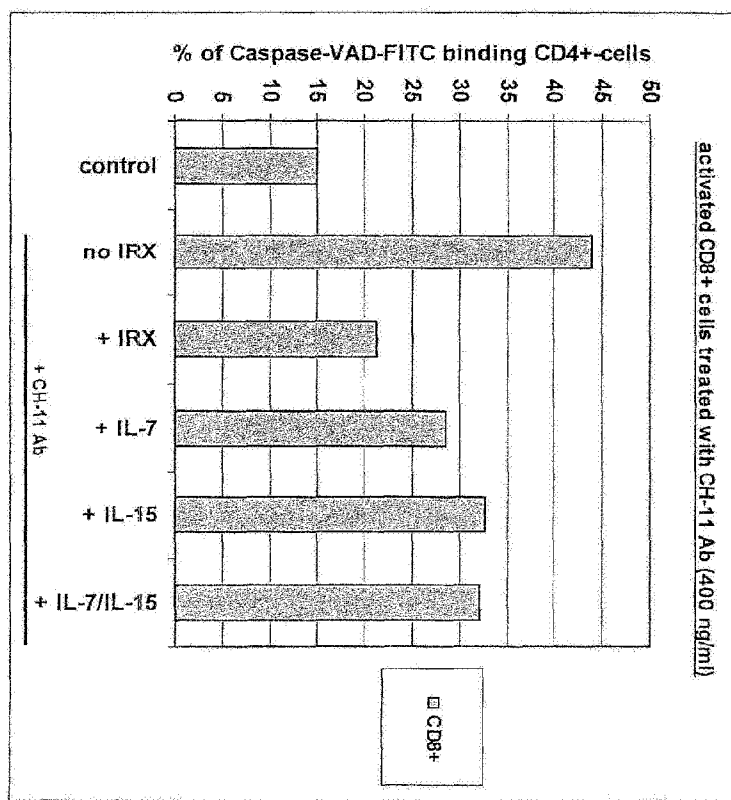


Figure 7

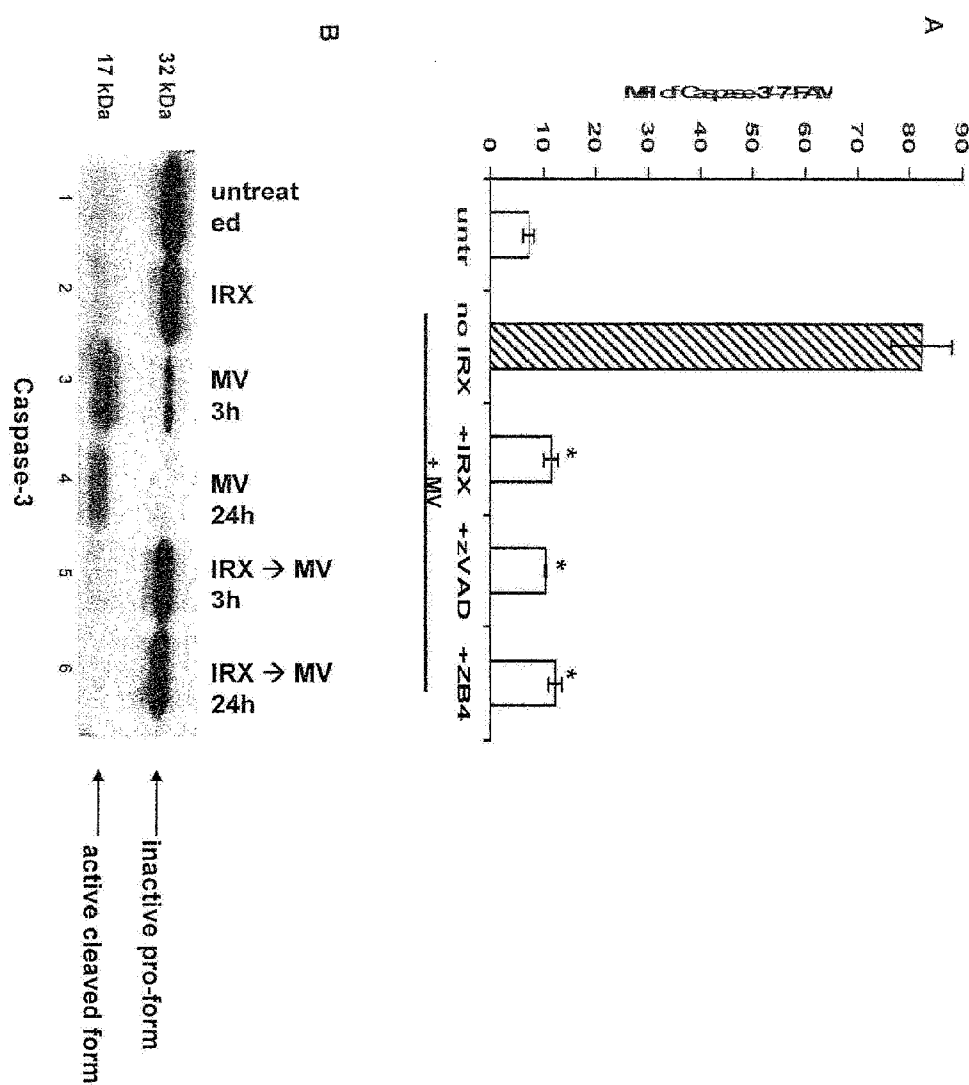


Figure 8

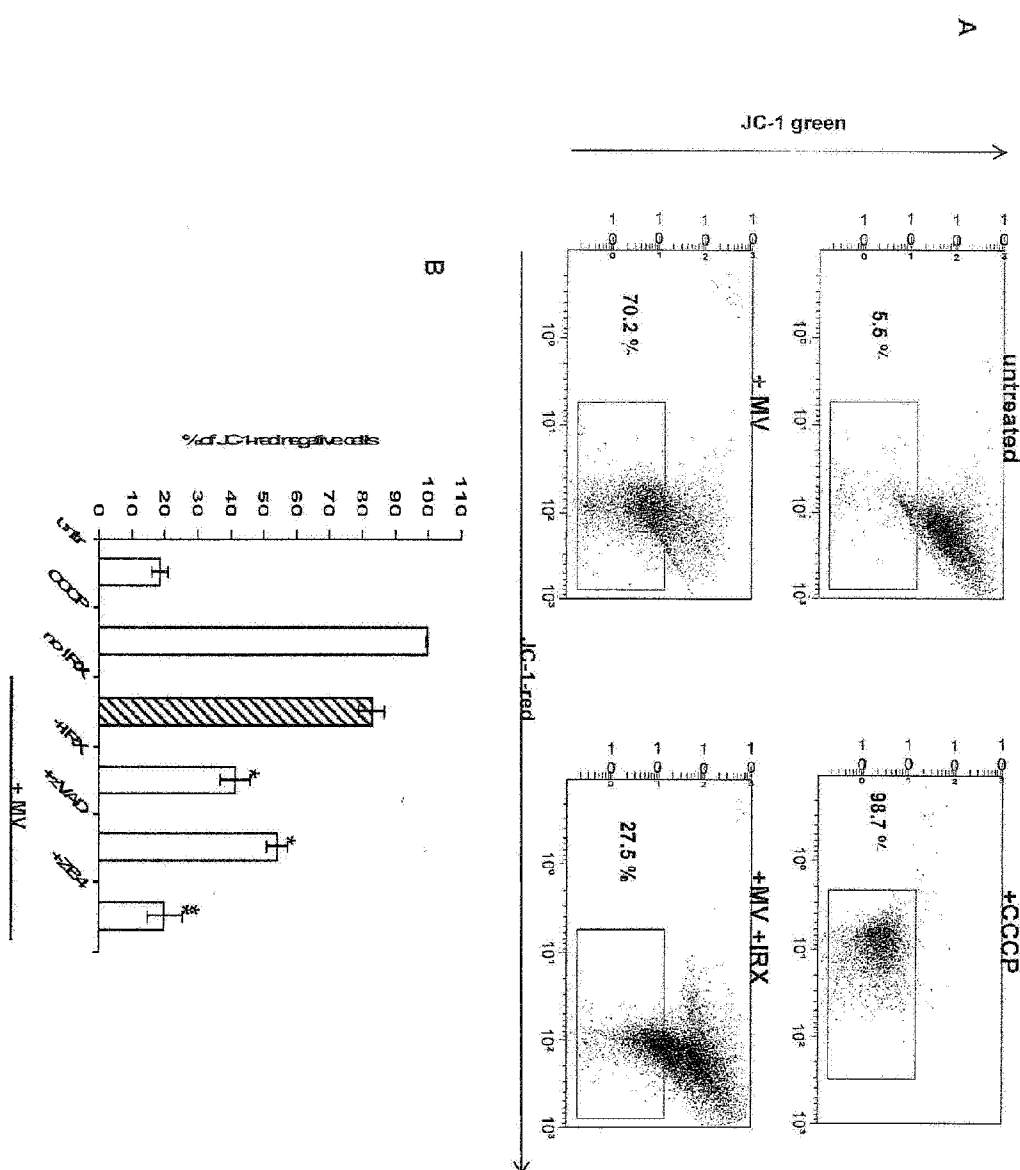
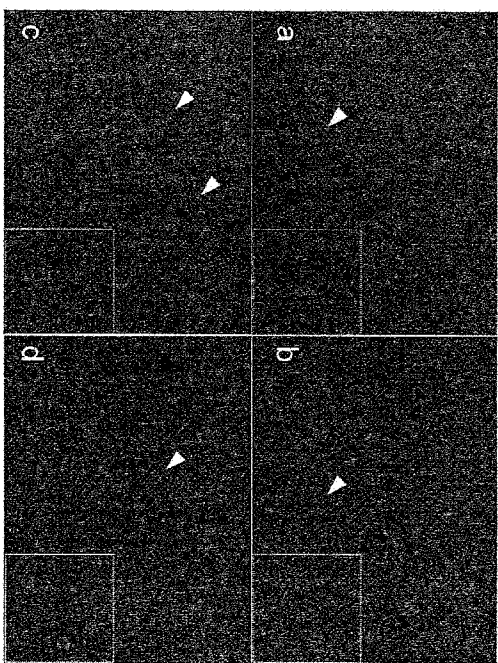


Figure 9



Mag x200, inserts x600

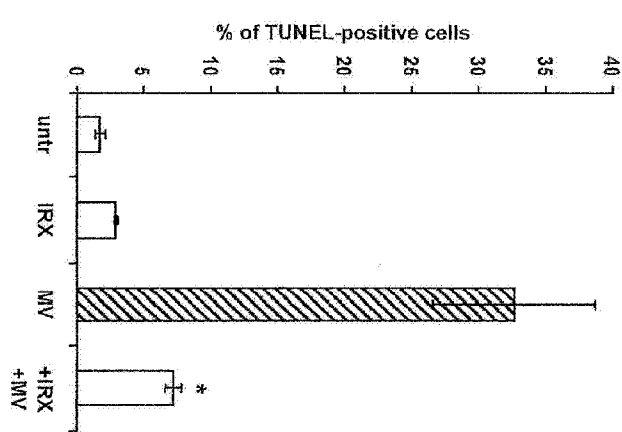


Figure 10

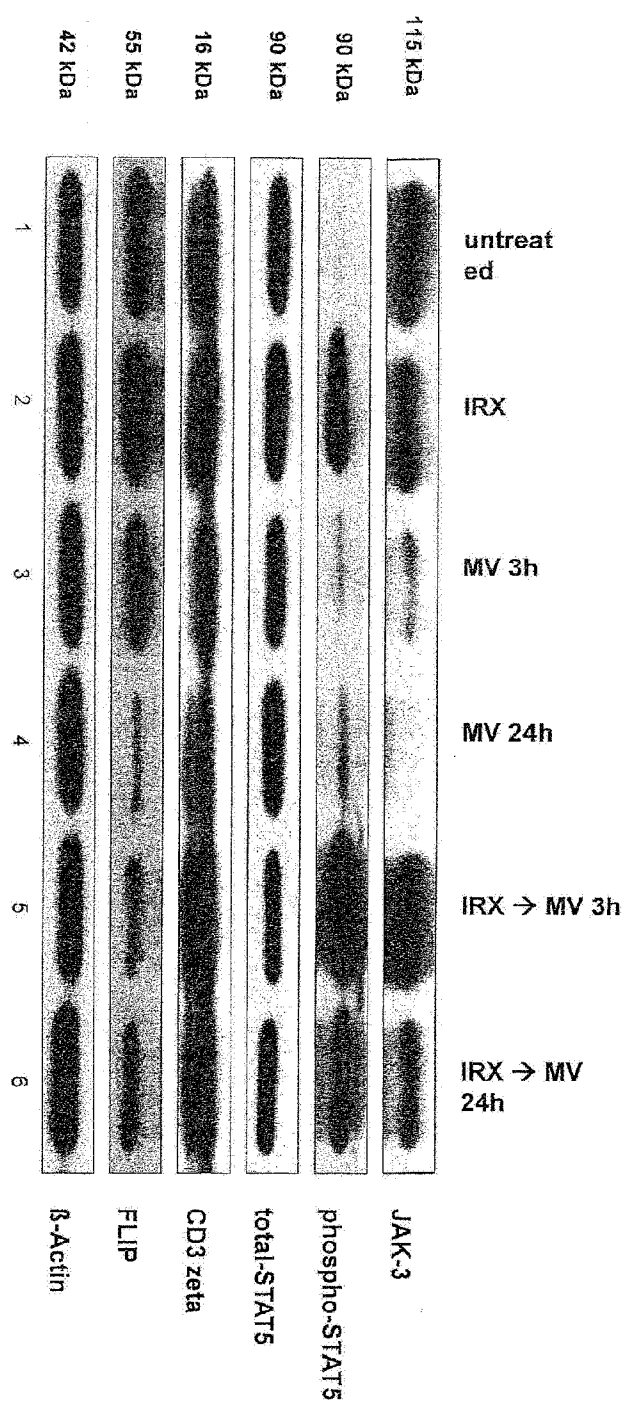


Figure 11A

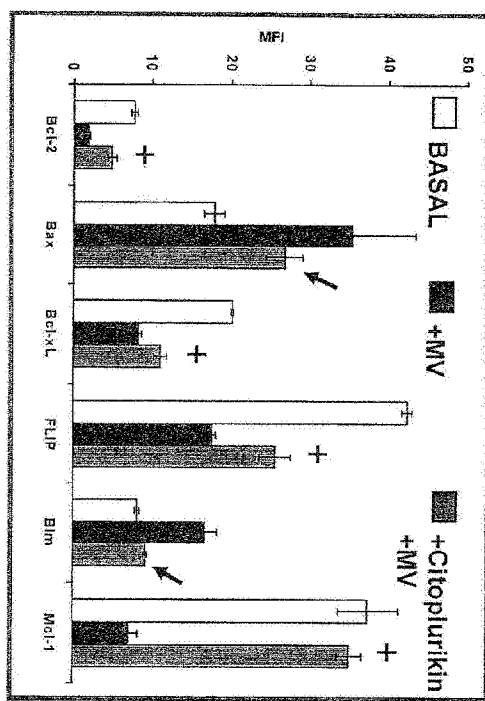


Figure 11B

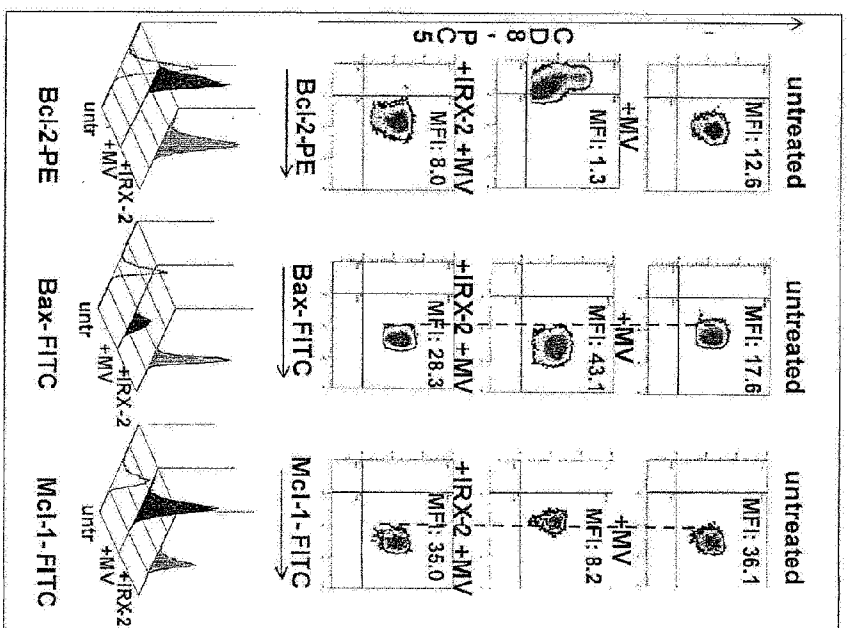


Figure 12

